

**The Dynamic Behavior of Macrophages in Wound Healing**

by

**MICHAEL KWAKU BOATENG**

Submitted in Partial Fulfillment of the Requirements

for the Degree of

MASTER OF SCIENCE

in

Mathematics

YOUNGSTOWN STATE UNIVERSITY

December, 2013

©

MICHAEL K. BOATENG

2013

## ABSTRACT

The first line of protection against infection for the human body is the skin. A break in this line of defense is called a wound. After the protective barrier is broken, the process of wound healing starts without delay. Wound healing is complex and dynamic. Most of the time wounds progress through phases depending upon the internal and external forces at work within the patient. Wound healing progresses through four phases. They are hemostasis, inflammation, proliferation and remodeling. This study describes a mathematical model which gives a possible explanation to the role and importance of macrophage phenotypes  $M_1$ : inflammatory macrophages,  $M_2$ : repair macrophages and  $M_R$ : regulatory macrophages during the inflammatory phase of wound healing. Six differential equations were formulated and solved numerically. The model results suggest that  $M_1$  macrophages are the first macrophage phenotype to enter into the wound and the decrease in the amount of these macrophages after inflammatory phase is a good sign that the wound is healing normally. Also, the imbalance between pro-inflammatory macrophages and repair macrophages is not damaging to the wound provided there is sufficient interleukin-10 (IL-10) in the wound. The model result also indicates that  $M_R$  macrophage phenotype is very important during the inflammatory phase of wound repair since they secrete IL-10 which inhibits pro-inflammatory macrophages. As a result, a possible explanation is offered as to how wounds can be stalled at the inflammatory phase of wound healing.

## ACKNOWLEDGEMENTS

This thesis would not have been possible without the guidance and the help of several individuals who in one way or another contributed immensely and extended their valuable assistance in the preparation and completion of this study. First and foremost, my utmost gratitude to Dr. A. Prieto Langarica from Department of Mathematics and Statistics-YSU (supervisor), Dr. Diana Fagan (immunology consultant) from Department of Biological Science -YSU and Dr. George Yates from Department of Mathematics and Statistics (committee member)-YSU.

Second, my appreciation go to all faculty, staff members and all graduate students of Department of Mathematics and Statistics-YSU for the motivation and encouragement you gave me during start and finish of this study.

# Contents

<b>1</b>	<b>Introduction</b>	<b>1</b>
1.1	Hemostasis Phase . . . . .	1
1.2	Inflammatory Phase . . . . .	2
1.3	Proliferation Phase . . . . .	3
1.4	Remodeling Phase . . . . .	4
1.5	Types of wounds . . . . .	4
1.6	The role of macrophages in wound healing . . . . .	5
<b>2</b>	<b>Mathematical Model</b>	<b>7</b>
2.1	The mathematical model . . . . .	11
2.2	Model equations . . . . .	13
2.2.1	$M_1$ macrophage . . . . .	13
2.2.2	$M_2$ macrophage . . . . .	14
2.2.3	$M_R$ macrophage . . . . .	15
2.2.4	Tumor necrosis factor(TNF) . . . . .	15
2.2.5	Transforming growth factor- $\beta$ (TGF- $\beta$ ) . . . . .	15
2.2.6	Interleukin- 10 (IL-10) . . . . .	16
<b>3</b>	<b>Steady State Solutions</b>	<b>17</b>
3.1	Calculated Steady State Solutions . . . . .	19
<b>4</b>	<b>Numerical solution of equations</b>	<b>22</b>
<b>5</b>	<b>Results and Discussion</b>	<b>34</b>
<b>6</b>	<b>Conclusion</b>	<b>38</b>

# 1 Introduction

A wound, in normal skin, is an injury that occurs when the protective barrier between the outermost layer (epidermis) and inner or deeper layer (dermis) is broken [8, 18]. After the protective barrier is broken, the process of wound healing starts without delay. Wound healing is a natural and complex process in which the body repairs itself after injury. It is thought to progress through four phases. These phases are hemostasis, inflammation, proliferation and remodeling [11].

## 1.1 Hemostasis Phase

When the body tissue sustains an injury, the body starts to bleed, thus losing blood. The first reaction of the body is to stop the bleeding by keeping the blood within the damaged blood vessels. This process is called hemostasis. There are three steps involved during hemostasis and they happen in rapid sequence [14, 12]. First, the blood vessels shrink to allow less blood to be lost. Second is the formation of a platelet plug. The blood that streams into the wound carries platelets. Platelets are small colorless disk-shaped cell fragments without a nucleus and they are found in large numbers in the blood. During hemostasis, platelets aggregate to form a temporary seal to serve as a cover for the wall of broken vessels. Platelets that stick to the collagen fibers of the wound become stickier. They then start producing chemicals such as adenosine diphosphate (ADP), serotonin and thromboxane A<sub>2</sub> [17]. These chemicals cause more platelets to aggregate creating a platelet plug which prevents further blood lost. Third is blood clotting (coagulation). Blood that flows into the wound also contains fibrinogen. Fibrinogen is a protein in the blood plasma that is essential for the thickening of blood. When fibrinogen is converted into fibrin (an insoluble protein that is produced during bleeding), clots are formed. The fibrin forms something like a mesh that acts as a glue for the sticky platelets. The fibrin mesh reinforces the platelet plug by trapping the platelets. Coagulation helps to close and maintain the platelet plug in wounds [9]. Platelets that are trapped in the wound by the fibrin mesh release chemical stimuli, such as platelet derived growth factor (PDGF), transforming growth factor- $\beta$  (TGF- $\beta$ ) and vascular

endothelial growth factor (VEGF). These growth factors are very useful in the subsequent phases of wound healing [7]. However, TGF- $\beta$  is a chemical that influences wound healing from the hemostasis phase to the remodeling phase of wound healing. Activated TGF- $\beta$  stimulates the rapid migration of neutrophils and monocytes to the wound site [10]. These events comprise the hemostasis phase and, in normal wounds, typically last a matter of hours [9]

## 1.2 Inflammatory Phase

After hemostasis, the inflammatory phase begins. Mast cells (cells found in the connective tissue) are activated and start discharging histamine, cellular particles (granules filled with enzymes), and other nitrogen compounds, such as ethylamine. Histamine is an organic nitrogen compound that makes the capillaries more permeable allowing the passage of white blood cells and some proteins, to allow them to engage pathogens in the infected tissues. The specific signs of inflammation around the wound site, such as *rubor* (redness), *calor* (heat), *tumor* (swelling) and *dolor* (pain) [15, 18], come about as a result of these mediators. Inflammation brings more blood, containing white blood cells, to the wound site. Neutrophils, granular white blood cells that are highly destructive to microorganisms, are the major cell type present in the wound 24-36 hours after injury. Chemokines are regulatory proteins produced in response to inflammatory stimuli. They activate white blood cells, bringing neutrophils to the wound site. The migration of neutrophils from the circulating blood into the wound site is guided by chemokines and other chemotactic agents such as TGF- $\beta$ , formylmethionyl peptides produced by bacteria, and others [15]. Neutrophils are attracted into the wound by the chemoattractants already released within 24 hours of injury and start eating up (phagocytosing) foreign particles, bacteria and blood clots [9, 13].

The largest white blood cells, monocytes, are also attracted into wound from the neighboring blood vessels by TGF- $\beta$  which is produced by platelets [9]. Monocytes differentiate into macrophages. Macrophages are essential in wound healing, since they are involved in the formation of new blood vessels, (angiogenesis), covering of the wound (epithelialization) and matrix deposition. Macrophages actively migrate into the wound in response to

a chemoattractant, such as TGF- $\beta$ , consuming the dead cells and tissue in their path, including dead neutrophils. These macrophages regulate wound healing by producing growth factors such as TGF- $\beta$ , tumor necrosis factor (TNF), Interleukin-10 (IL-10) and others, like macrophage derived growth factor (MDGF), vascular endothelial growth factor (VEGF), endothelial growth factor (EGF) and platelet derived growth factor (PDGF) [9]. Growth factors are chemicals made by cells that act on other cells to stimulate cellular growth and proliferation. The growth factors like TGF- $\beta$ , TNF, and IL-10 are very important growth factors during the inflammatory phase of wound healing, because they act as signaling molecules between cells and also stimulate the proliferation of the various macrophage phenotypes. MDGF, VEGF, EGF and PDGF are responsible for the migration of fibroblasts from the surrounding undamaged extracellular matrix into the wound. Therefore, they are useful for the proliferation phase of wound healing. Fibroblasts are cells that give rise to connective tissue and synthesize collagen. They are also the major cells within the proliferative phase of wound healing. The migration of fibroblasts into the wound site leads to the proliferation phase of wound healing. The inflammation phase lasts for three days [6, 1].

### **1.3 Proliferation Phase**

The proliferative phase starts on the third day after the initial injury and lasts for about 2 weeks. It consists of fibroblast migration into the wound site, accumulation of newly synthesized extracellular matrix and an abundant formation of granulation tissue (new connective tissue and tiny blood vessels that are formed on the surface of a wound during the healing process) [15]. Fibroblasts are the major cells involved in the proliferation phase of wound healing. Fibroblasts move into the wound after pro-inflammatory macrophages have left the wound site [9]. Chemoattractants, such as PDGF, attract fibroblasts into the wound. These fibroblasts produce collagen, which is a major component of the extracellular matrix. Matrix metalloproteinases (MMPs) are enzymes that play an important role in the control of signals produced by matrix molecules which regulate cell death and growth. They are produced by activated neutrophils, macrophages and fibroblasts. They break



down the collagen and other extracellular matrix proteins, creating a granular foundation for the wound. The formation of new blood vessels (angiogenesis) provides the "conduits" for further cell migration towards the center of the wound. The growth factors in the wound activate the keratinocytes (epidermal cells that produce keratin) to migrate into the wound and proliferate. They cover the top of the wound by creating an epithelial layer [9, 25]. Peripheral keratinocytes move into the wound to provide an external coverage for the wound. Fibroblasts and endothelial cells (cells that form the lining of blood and lymph vessels and the inner layer of the endocardium) are the primary cells involved in the proliferation phase. This is because fibroblasts give rise to connective tissue and synthesize collagen, and endothelial cells help in the formation of new blood vessels [11].

#### **1.4 Remodeling Phase**

During this phase, the remodeling of the collagen matrix is completed, full wound contraction occurs and the strength of the wound increases significantly. Normally it increases from 20% of normal tensile strength to 80% within a period of two years [9]. The most important growth factors that regulate this process are PDGF, TGF- $\beta$  and fibroblast growth factors (FGFs). These growth factors are produced by macrophages and fibroblasts. At the final stage of wound healing the density of fibroblasts and macrophages is reduced. This is due to the fact that the cells naturally die (apoptosis) [17]. As time goes by, the growth of capillaries stops, there is a significant decrease in blood flow to the wound area and metabolic activity decreases [15]. This results in a fully healed wound. The remodeling phase may last 1-2 years or more [9, 20].

#### **1.5 Types of wounds**

Wound healing can be classified as chronic or acute, based upon the time it takes to heal [25]. Acute wounds are wounds that heal with no complications in a predicted amount of time. It is thought that acute wounds progress through the four phases of wound healing. [9, 21].

Chronic wounds are wounds that are stuck in one or more phases of wound healing and these are a huge socioeconomic problem [9]. People with a chronic wound encounter a lot of pain, immobility and bad quality of life. It is projected that it costs about 3 billion US dollars to treat the symptoms of leg ulceration (chronic wound) each year. In addition, there are 2 billion US dollars in cost associated with lost work days, for people with this problem every year. Typical of chronic wounds is that they take longer time to heal and many wounds do not heal at all [25, 4]. There are four main categories of chronic wounds: arterial wounds (they occur as result of insufficient blood supply), pressure wounds (which occur over a bony prominence as a result of pressure), venous wounds (which are commonly located above the ankle and below the knee) and diabetic wounds (wounds associated with diabetes) [8, 9]. The lower limbs of patients with non-healing wounds, such as pressure, arterial and diabetic are often amputated because medical personnel are left with no other options.

## 1.6 The role of macrophages in wound healing

Within 2 days after wounding, the growth factor, TGF- $\beta$ , attracts macrophages into the wound [22]. They start eating up the dead cells and tissue in the wound, including dead neutrophils. These macrophages also control wound healing through the production of TGF- $\beta$ , TNF, IL-10 and others like MDGF, VEGF, EGF and PDGF [9]. Macrophages are also important during the proliferation phase of wound healing because they produce growth factors such as PDGF and TGF- $\beta$  which attract fibroblasts into the wound [7, 19]. Fibroblasts produce collagen, which is a major component of the extracellular matrix. PDGF and TGF- $\beta$ , produced by macrophages and fibroblasts, regulate the remodeling of the wound by increasing the collagen content in the wound [5].

Monocytes differentiate into  $M_1$  (pro-inflammatory) macrophages in the presence of interferon  $\gamma$  (IFN  $\gamma$ ) and differentiate into  $M_2$  and  $M_R$  (regulatory) macrophages in the presence of interleukin 4 and 13 (IL-4, IL-13) [16]. Each macrophage phenotype produces different growth factors and cytokines and has a different role in wound healing. Cytokines are proteins made by cells and they act on other cells to promote or hinder their functions. The first macrophage phenotype to appear in the wound after neutrophils are the  $M_1$

macrophages [21]. They are believed to produce mediators that cause inflammation, for example TNF, nitric oxide (NO), and IL-1, IL-12 and IL-23. These mediators activate the various antimicrobial mechanisms that help in killing invading microorganisms. However, these mediators can also damage the neighboring tissues and lead to abnormal inflammation.  $M_1$  macrophages are believed to play a key role in chronic inflammation and therefore their responses to pro-inflammation and microorganism destruction must be controlled to avoid extensive tissue damage. When the inflammatory stimulus or pathogen is eliminated,  $M_1$  cell stimulation decreases [8, 16].  $M_2$  and  $M_R$  (regulatory) macrophages start increasing in the wound, to promote wound healing [16].  $M_2$  macrophages produce growth factors such as TGF- $\beta$  and PDGF that increase epithelial cell and fibroblast activity.  $M_2$  derived TGF- $\beta$  contributes to tissue regrowth and wound repair by promoting fibroblast differentiation into myofibroblasts (fibroblasts having some of the characteristics of smooth muscle cells) [16].  $M_2$  derived PDGF stimulates MMP activity in the wound [25, 22, 18]. They also produce factors that induce myofibroblasts to die, which may be important for wound repair, since excessive numbers of myofibroblasts may lead to excessive scarring. In the final stages of wound healing, macrophages possess the characteristics of regulatory (suppressive) macrophages ( $M_R$  macrophages).  $M_R$  macrophages produce IL-10, arginase-1 (ARG-1), resistin-like molecule  $\alpha$  (REL- $\alpha$ ) and programmed death ligand 2 (PDL2). IL-10 inhibits  $M_1$  macrophages, which is important for wound healing because excessive  $M_1$  macrophages may lead to chronic inflammation. ARG-1, REL $\alpha$  and PDL2 promote wound repair by limiting the development of scar (fibrosis) and collagen synthesis by activated myofibroblasts [16].

To better understand the causes of chronic wounds it is important to understand first the process of normal wound healing. The objective of this paper is to examine the inflammatory phase of wound healing. The focus will be on macrophage population behavior and how the macrophage phenotypes  $M_1$ ,  $M_2$  and  $M_R$  influence the inflammatory phase of the wound healing process.

## 2 Some previous work on wound healing

There have been some mathematical models of wound healing. These models have so far been focused on the proliferation and the repair stages of the wound healing process. Some mathematical models of diabetic wound healing have been developed and they were directed towards the inflammatory phase of wound healing. This study is relevant to these papers in many ways. Helen V. Waugh and Jonathan A. Sherratt described mathematical models which give a possible explanation for diabetic wound healing by just looking at the inflammatory phase of wound healing. To better understand diabetic wound healing, one needs to clearly understand the role that macrophages play during the inflammatory stage of normal wound healing so that possible hypothesis can arise to explain what can go wrong in diabetic wounds. The other papers look at the healing of both infected and uninfected wounds and the role of collagen in wound healing. Neutrophils and macrophages are responsible for bacteria elimination from the wound and this occurs during the inflammatory phase of wound healing. So for deeper understanding of wound infection, it is important to understand the role of macrophages regarding bacteria elimination from the wound. Collagen is produced by fibroblasts during the proliferation stage of wound healing and fibroblasts are attracted into the wound by growth factors such as MDGF, VEGF, EGF and PDGF. These growth factors are produced during the inflammatory stage of wound healing by macrophages. Therefore, the role of macrophages in wound healing is important in the healing process. Macrophages are highly present during the inflammatory phase and this is the main reason why our study focuses on the inflammatory phase of wound healing.

The mathematical model of diabetic wound healing described by Helen V. Waugh and Jonathan A. Sherratt [25] gives a possible explanation for the disruption in diabetic wounds. They suggest that the distribution of macrophage phenotypes in the diabetic patient is altered, when compared to normal wound repair. Among the four phases of the wound healing process, their work focuses on the inflammatory phase of wound healing since this is when macrophages are most involved. The model consisted of three variables: inflammatory macrophage, repair macrophage and TGF- $\beta$  concentrations. Three differential equations

involving these variables and other parameters were formulated and solved numerically. The results of the model confirmed the hypothesis that the stability of the macrophage phenotypes is disrupted in diabetic wound healing. Their work highlighted the importance of the macrophage in diabetic wound healing and supported the hypothesis that diabetic wounds appear to be stalled in the inflammatory phase of the wound healing process and the wound can be ‘jump-started’ into healing by applying the suitable treatment.

Waugh, Helen V., and Jonathan A. Sherratt [24] also presented a mathematical model of wound healing in both normal and diabetic wounds focusing on the effects of adding engineered skin substitute therapies to the wound (Apligraf and Dermagraft). The variables used in the model were inflammatory macrophages, repair macrophages, TGF- $\beta$  concentrations, concentration of PDGF, density of fibroblasts, density of collagen and the concentration of hyaluronan. Seven differential equations were formulated and solved numerically. The results of the model are as follows: First, the macrophage population persists longer in the diabetic wound that are not treated than in the normal wound. Also, there are significantly more inflammatory macrophages than repair macrophages. Second, there are lower amounts of hyaluronan in the diabetic wound than in the normal wound. Hyaluronan levels were even much lower than what is usually found in normal skin. This leads to a non-healing wound, as small amounts of monocytes differentiate into repair macrophages and so there is a disruption in the distribution of the macrophage phenotype. Third, in this model, treating a wound with PDGF in amounts normally found in wounds does not bring about healing, although healing occurs when very large amounts of PDGF are used. Treating wounds with hyaluronan alone in large amounts does induce wound healing. Large quantities of hyaluronan implies that large amounts of monocytes differentiate into repair macrophages and less monocytes differentiate into macrophages that cause inflammation, thus solving the problem of the macrophage phenotype imbalance seen in the untreated diabetic wound. Adding fibroblasts alone to the wound also encouraged healing. Large amounts of fibroblasts implies that there is an increase in hyaluronan synthesis and this corrects the imbalance in the distribution of the macrophage phenotype, as described above. In conclusion, the model found that the main element in the Apligraf and Dermagraft

additives affecting wound healing is hyaluronan.

Because one can best understand the disruption in chronic wounds when the role that macrophages play in the inflammatory phase of normal wound healing is clearly understood, it is therefore important to investigate the activities of macrophages in normal wounds, which is the aim of our study. Waugh, Helen V., and Jonathan A. Sherratt described a mathematical model that focuses on the inflammatory phase of wound healing process. Our model also focuses on the inflammatory phase of wound healing. Both works investigate the activities of macrophages during the inflammatory phase. However, there is difference between their model and our model, as they only examined two macrophage phenotypes (inflammatory and repair macrophages) as variables in their model, whereas in our model we included three macrophage phenotypes as variables. Also, TGF- $\beta$  is the only growth factor (cytokine) that was considered in their model whereas in our model, there are three important chemicals (cytokines): TGF- $\beta$ , IL-10 and TNF, as they play a very crucial role in wound healing during the inflammatory phase. IL-10 is secreted by  $M_R$  macrophages and it inhibits the  $M_1$  macrophages (pro-inflammatory macrophages). TNF is produced by  $M_1$  macrophages and it stimulates  $M_1$  macrophages, which can be damaging to the healing process if it is not regulated. Studying the interaction between these macrophages and the respective chemicals they produce is an important focus of our model.

The work of E. Agyingi, S. Maggelakis and D. Ross [2] presents a mathematical model of the healing of both infected and uninfected wounds. Their work investigates whether infection is affected more by bacterial density or by bacteria virulence. The model accounted for whether or not capillary regeneration is dependent on the availability of oxygen and for the production of growth factors for both non-contaminated and contaminated wounds. The model consisted of four variables: concentration of oxygen in the wound, the concentration of macrophage-derived growth factors (MDGFs), the capillary density and bacterial density. Four nonlinear reaction-diffusion equations were formulated and solved numerically. Three different results were obtained from the model. First, the model indicates that where there are low oxygen concentrations there is increased production of MDGFs and this leads to the migration of capillaries into the wound. The regeneration of capillaries brings in more

oxygen, which then lowers the production of MDGFs. That is, the wound heals successfully and in a timely manner in the absence of bacteria. Second, when the density of non-virulent bacteria is low or high the wound also heals successfully and in a timely manner. Third, when the density of virulent bacteria is low or high the wound stalls as time progresses. In conclusion, bacteria virulence determines whether a wound becomes infected, not bacteria concentration.

Our study is related to the work done by E. Agyingi, S. Maggelakis and D. Ross, since wound infection occurs as a result of bacteria invasion of the wound. Macrophages are responsible for bacteria elimination from the wound after neutrophils die. Therefore, to better understand wound infections, it is important to understand the role of macrophages regarding bacteria elimination from the wound and which macrophage phenotype is important for the elimination of bacteria from the wound. Our work is therefore relevant to their study since one needs to understand the inflammatory phase of wound healing to better understand what causes infection in wounds.

The work of Segal, Rebecca A *et al* [21] presents a mathematical model of collagen accumulation as a marker for wound healing. Their model is a system of differential equations which tracks fibroblasts, collagen, inflammation, and pathogens. The model was validated by comparing the appropriate activities for the inflammatory, proliferative and remodeling phases of wound healing. Subsequent validation was made by comparison to collagen accumulation experiments by Madden and Peacock 1971. The model was then used to investigate the impact of local oxygen levels on wound healing and confirmed that oxygen plays important role in successful wound healing. Finally a comparison of two wound healing therapies, antibiotics and increased fibroblast proliferation, were presented. The model finds that the antibiotics treatment is only effective while pathogens are present and that the fibroblast treatment is effective throughout the healing process and brings about wound closure in low oxygen environment.

Collagen is produced by fibroblasts during the proliferation stage of wound healing and fibroblasts are attracted into the wound by growth factors such as MDGF, VEGF, EGF and PDGF. These growth factors are produced during the inflammatory stage of wound

healing by macrophages. This implies that for one to really understand the proliferation and remodeling stages of wound healing, which absolutely depend upon the role of macrophages at the inflammatory phase, there is a need to know the activities of macrophages during the inflammatory phase and that is what this study explains.

The work of Helen V. Waugh and Jonathan A. Sherratt [25] suggests that monocytes differentiate into inflammatory macrophages in the presence of 1,3- $\beta$  glucan, repair macrophages in the presence of hyaluronan and cytotoxic macrophage in the presence of polyinosinate-polycytidylylate. However, a recent publication (2011) on monocytes and macrophages by Peter J Murray and Thomas A. Wynn [16], indicates that monocytes differentiate into  $M_1$  macrophages in the presence of interferon- $\gamma$  (IFN- $\gamma$ ) and differentiate into  $M_2$  and  $M_R$  (regulatory) macrophages in the presence of interleukin 4 and 13 (IL-4, IL-13). The objective of this paper is to use the current literature on monocyte and macrophage differentiation to update previous mathematical models to investigate the inflammatory phase of wound healing. Therefore, this study describes a mathematical model that describes the inflammatory phase of wound healing process with particular attention to macrophage phenotypes in the hope that we can better understand disruptions in the wound healing process.

## 2.1 The mathematical model

The focus of this study will be on macrophage population behavior and how the macrophage phenotypes,  $M_1$ ,  $M_2$  and  $M_R$ , influence the inflammatory phase of the wound healing process. By only looking at this phase of wound healing process we are able to exclude fibroblasts and endothelial cells from the model, as fibroblast and endothelial cells come into the wound site during the proliferation phase of wound healing following the inflammatory phase.



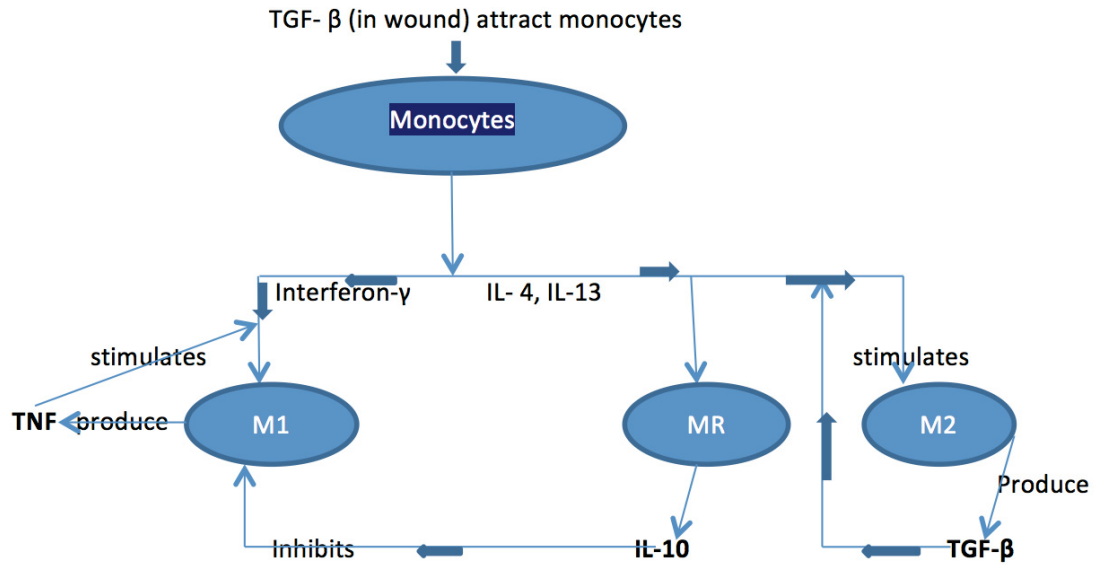


Figure 1: Flow chart showing the interaction among macrophage phenotypes and the respective cytokines (chemicals) that they produce. This flow chart was made based on the publication by Peter J Murray and Thomas A. Wynn [16].

The model consists of six variables and six differential equations. The following variables were chosen: the density of  $M_1$  macrophages:  $M_1(t)$  ( $cells\ mm^{-3}$ ), the density of  $M_2$  macrophages:  $M_2(t)$  ( $cells\ mm^{-3}$ ) and the density of  $M_R$  macrophages:  $M_R(t)$  ( $cells\ mm^{-3}$ ). These are the key cell populations during the inflammatory phase. Furthermore, the concentration of TNF:  $T_N(t)$  ( $pg\ mm^{-3}$ ), the concentration of TGF- $\beta$ :  $T_G(t)$  ( $pg\ mm^{-3}$ ) and the concentration of IL-10 :  $IL(t)$  ( $pg\ mm^{-3}$ ) were included because TNF (produced by  $M_1$  macrophages) stimulates  $M_1$  macrophages, TGF- $\beta$  (produced by platelets and  $M_2$  macrophages) stimulates  $M_2$  macrophages and causes the migration of monocytes into the wound and IL-10 (produced by  $M_R$  macrophages) inhibits  $M_1$  macrophages. All the variables above are functions of  $t$ , where  $t$  represents time in days. <sup>1 2</sup>

<sup>1</sup>Figure 1 illustrates the interaction among the macrophage phenotypes and the respective chemicals that they produce. Monocytes are attracted into the wound by TGF- $\beta$  and differentiate into  $M_1$  macrophage in the presence of interferon- $\gamma$  (IFN- $\gamma$ ) and differentiate into  $M_2$  and  $M_R$  (regulatory) macrophages in the presence of interleukin 4 and 13 (IL-4, IL-13).  $M_1$  produce TNF and TNF stimulates  $M_1$  macrophages.  $M_R$  produce IL-10 and IL-10 inhibits  $M_1$  macrophages.  $M_2$  macrophage produce TGF- $\beta$ , which stimulates  $M_2$  macrophages.

<sup>2</sup>These assumptions in the flow chart were made based on the publication by Peter J Murray and Thomas A. Wynn [16]

## 2.2 Model equations

A system of ordinary differential equations is used to model the inflammatory phase of wound healing. The equations for the  $M_1$ ,  $M_2$  and  $M_R$  macrophages were determined using:

Rate of change of cell population is equal to the amount of cells that migrate into the wound plus cell reproduction at the wound site minus the amount of cells that die or leave the wound [25]. Also, the equations for TGF- $\beta$ , TNF and IL-10 were determined using:

Rate of change of chemical concentration is equal to the concentration of chemical produced by cells minus the amount of chemical decaying [24].

### 2.2.1 $M_1$ macrophage

$$\frac{dM_1}{dt} = \alpha A(T_G) + bT_N M_1 - cILM_1 - d_1 M_1 \quad (1)$$

This differential equation represents the change in  $M_1$  macrophages.  $\frac{dM_1}{dt}$  represents the rate of change in  $M_1$  macrophages in the wound. The term  $\alpha A(T_G)$  represents the increase in density of  $M_1$  macrophages due to monocytes migration to the wound by TGF- $\beta$ . The function  $A(T_G)$  represents the migration of monocytes to the wound site in response to TGF- $\beta$  concentration at the wound site. The function  $A(T_G)$  is given by  $A(T_G) = -2.47T_G^3 + 21.94T_G^2 + 6.41T_G + 1.75$  [23]. The plot of this cubic function is shown in Figure 2. The plot shows that monocytes migration is small but positive when  $T_G = 0$  and maximum migration of monocytes is reached when  $T_G = 6 \text{ pg mm}^{-3}$ . The parameter  $\alpha$  is the proportion of monocytes that differentiate into  $M_1$  macrophages and it is a non-dimensional parameter.  $M_1$  macrophages produce TNF and TNF stimulates  $M_1$  macrophages.

The term  $bT_N M_1$  represents the stimulation of  $M_1$  macrophages by TNF and the parameter  $b$  is the increasing rate of  $M_1$  by TNF concentration and its unit is  $(\text{pg mm}^{-3})^{-1} \text{day}^{-1}$ . IL-10 is produced by  $M_R$  macrophages and IL-10 inhibits  $M_1$  macrophages. The term  $cILM_1$  represents the reduction of  $M_1$  macrophages by the IL-10 and  $c$  is a parameter that represents the decreasing rate of  $M_1$  by IL-10 and its unit is  $(\text{pg mm}^{-3})^{-1} \text{day}^{-1}$ . Finally,

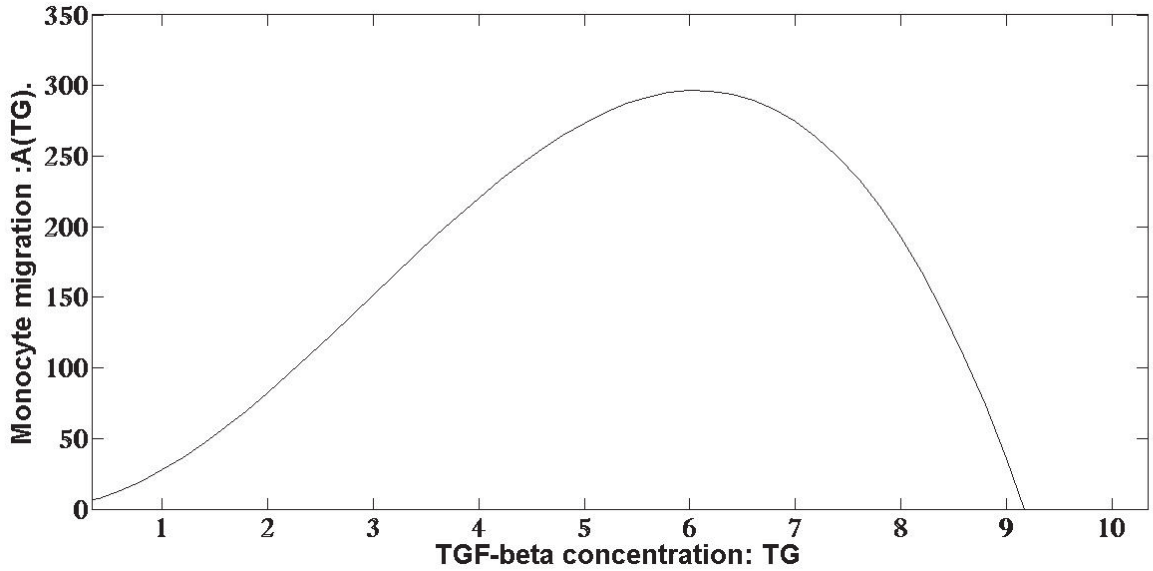


Figure 2: A qualitative form of the function  $A(T_G)$  depicting monocytes migration. Note that when  $T_G = 0$ , the macrophage migration is small but positive and maximum of monocytes is reached when  $T_G = 6$ . The figure is a plot of a cubic function  $A(T_G) = -2.47T_G^3 + 21.94T_G^2 + 6.41T_G + 1.75$

the term  $d_1M_1$  represents the departure or death of  $M_1$  macrophages from the wound site and  $d_1$  represents the dying rate of  $M_1$  macrophages at the wound site and its unit is  $day^{-1}$ .

### 2.2.2 $M_2$ macrophage

$$\frac{dM_2}{dt} = \beta A(T_G) + hT_G M_2 - d_2 M_2. \quad (2)$$

This differential equation represents the rate of change in  $M_2$  macrophages in the wound. The first term,  $\beta A(T_G)$ , represents the increase in density of  $M_2$  macrophages due to monocytes migration to the wound. The parameter  $\beta$  represents the proportion of monocytes that differentiate into  $M_2$  macrophage and it is dimensionless.  $M_2$  macrophages produce TGF- $\beta$ , which stimulates  $M_2$  macrophage growth and it is represented in the equation by  $hT_G M_2$  where  $h$  is the increasing rate of  $M_2$  macrophages by TGF- $\beta$  concentrations and its unit is  $(pg\ mm^{-3})^{-1} day^{-1}$ . The term  $d_2 M_2$  represents the departure or death of  $M_2$  macrophages in the wound where  $d_2$  is a parameter representing the dying rate of  $M_2$

macrophages at the wound site and its unit is  $day^{-1}$ .

### 2.2.3 $M_R$ macrophage

$$\frac{dM_R}{dt} = \gamma A(T_G) - d_3 M_R. \quad (3)$$

Equation (3) describes the rate of change in  $M_R$  macrophages in the wound. The first term  $\gamma A(T_G)$  represents the increase in density of  $M_R$  macrophages due to monocytes migration to the wound and the parameter  $\gamma$  (dimensionless) represents the proportion of monocytes that differentiate into  $M_R$  macrophages. The second term in the equation,  $d_3 M_R$ , represents the amount of  $M_R$  macrophages leaving or dying where the parameter  $d_3$  represents the dying rate of  $M_R$  macrophages and its unit is  $day^{-1}$ .

### 2.2.4 Tumor necrosis factor(TNF)

$$\frac{dT_N}{dt} = u M_1 - d_4 T_N. \quad (4)$$

Equation (4) is a differential equation that characterizes the rate of change in TNF concentration in the wound.  $M_1$  macrophages produce TNF. The first term,  $u M_1$ , represents the production of TNF by  $M_1$  macrophages and  $u$  is a parameter representing the rate of production of TNF by  $M_1$  macrophages and its unit is  $pg\ cell^{-1} day^{-1}$ . The last term  $d_4 T_N$  represents the decaying factor of TNF where  $d_4$  is parameter representing the decay rate of  $T_N$  concentration in the wound.

### 2.2.5 Transforming growth factor- $\beta$ (TGF- $\beta$ )

$$\frac{dT_G}{dt} = k M_2 - d_5 T_G. \quad (5)$$

This equation characterizes the rate of change in TGF- $\beta$  concentration in the wound.  $M_2$  macrophages produce TGF- $\beta$ . The first term represents the production of TGF- $\beta$  by  $M_2$

macrophages and  $k$  is a parameter representing the production rate of TGF- $\beta$  by  $M_2$  macrophages and its unit is  $pg\ cell^{-1}day^{-1}$ . The last term represents the decaying factor of TGF- $\beta$  where  $d_5$  is parameter representing the decay rate of TGF- $\beta$  concentration in the wound and its unit is  $day^{-1}$ .

### 2.2.6 Interleukin- 10 (IL-10)

$$\frac{dIL}{dt} = wM_R - d_6IL. \quad (6)$$

This differential equation characterizes the rate of change in IL-10 concentration in the wound.  $M_R$  macrophages produce IL-10. The first term,  $wM_R$ , represents the production of IL-10 by  $M_R$  macrophages and  $w$  is a parameter representing the production rate of IL-10 by  $M_R$  macrophages and its unit is  $pg\ cell^{-1}day^{-1}$ . The last term,  $d_6IL$ , represents the decaying factor of IL-10 where  $d_6$  is the parameter representing the decay rate of  $IL$  concentration in the wound.

The system of differential equations consists of six variables and 14 parameters. Since  $\alpha$ ,  $\beta$  and  $\gamma$  represent the proportions of monocytes that differentiate into  $M_1$ ,  $M_2$  and  $M_R$  macrophages respectively,  $\alpha + \beta + \gamma = 1$ .

### 3 Steady State Solutions

Setting equations (1) - (6) to zero, we have the following system of algebraic equations.

$$wM_R - d_6IL = 0 \quad (7)$$

$$kM_2 - d_5T_G = 0 \quad (8)$$

$$uM_1 - d_4T_N = 0 \quad (9)$$

$$\gamma A(T_G) - d_3M_R = 0 \quad (10)$$

$$\beta A(T_G) + hT_G M_2 - d_2M_2 = 0 \quad (11)$$

$$\alpha A(T_G) + bT_N M_1 - cILM_1 - d_1M_1 = 0 \quad (12)$$

Table 1 and 2 below shows the parameter values for the Figures 3- 12. The parameters have the same meaning as described in the model equations above.

Parameters	Figure 3	Figure 4	Figure 5	Figure 6	Figure 7
$\alpha$	1/3	0.4	0.5	0.5	0.6
$\beta$	1/3	0.3	0.25	0.3	0.2
$\gamma$	1/3	0.3	0.25	0.2	0.2
$b (pg \text{ mm}^{-3})^{-1} day^{-1}$	0.05	0.05	0.05	0.05	0.05
$c (pg \text{ mm}^{-3})^{-1} day^{-1}$	0.1	0.1	0.1	0.1	0.1
$h (pg \text{ mm}^{-3})^{-1} day^{-1}$	0.05	0.05	0.05	0.05	0.05
$u \text{ pg cell}^{-1} day^{-1}$	1	1	1	1	1
$k \text{ pg cell}^{-1} day^{-1}$	0.07	0.07	0.07	0.07	0.07
$w \text{ pg cell}^{-1} day^{-1}$	2	2	2	2	2
$d_1 \text{ day}^{-1}$	0.2	0.2	0.2	0.2	0.2
$d_2 \text{ day}^{-1}$	0.2	0.2	0.2	0.2	0.2
$d_3 \text{ day}^{-1}$	0.2	0.2	0.2	0.2	0.2
$d_4 \text{ day}^{-1}$	8.5	8.5	8.5	8.5	8.5
$d_5 \text{ day}^{-1}$	9.1	9.1	9.1	9.1	9.1
$d_6 \text{ day}^{-1}$	7.3	7.3	7.3	7.3	7.3

Table 1: Parameter values for all Figures 3- 7.

Parameters	Figure 8	Figure 9	Figure 10	Figure 11	Figure 12
$\alpha$	0.6	0.7	0.7	0.05	0.02
$\beta$	0.15	0.15	0.01	0.9	0.9
$\gamma$	0.25	0.15	0.29	0.05	0.08
$b (pg mm^{-3})^{-1} day^{-1}$	0.05	0.05	0.05	0.05	0.05
$c (pg mm^{-3})^{-1} day^{-1}$	0.1	0.1	0.1	0.1	0.1
$h (pg mm^{-3})^{-1} day^{-1}$	0.05	0.05	0.05	0.05	0.05
$u pg cell^{-1} day^{-1}$	1	1	1	1	1
$k pg cell^{-1} day^{-1}$	0.07	0.07	0.07	0.07	0.07
$w pg cell^{-1} day^{-1}$	2	2	2	2	2
$d_1 day^{-1}$	0.2	0.2	0.2	0.2	0.2
$d_2 day^{-1}$	0.2	0.2	0.2	0.2	0.2
$d_3 day^{-1}$	0.2	0.2	0.2	0.2	0.2
$d_4 day^{-1}$	8.5	8.5	8.5	8.5	8.5
$d_5 day^{-1}$	9.1	9.1	9.1	9.1	9.1
$d_6 day^{-1}$	7.3	7.3	7.3	7.3	7.3

Table 2: Parameter values for all Figures 8- 12.

<sup>3 4 5</sup> From equation (8) and (10),  $M_1$  and  $M_R$  can be solved from equation (10) and equation (10) to give.

$$M_2 = \frac{d_5 T_G}{k}, \quad M_R = \frac{\gamma A(T_G)}{d_3}. \quad (13)$$

Using equation for  $M_R$ , from equation (13), and equation (7), we find equation for  $IL$  which is given in equation (14)

$$IL = \frac{w\gamma A(T_G)}{d_3 d_6}. \quad (14)$$

From equation (12) and (9), we find  $M_1$  and  $T_N$  respectively,

$$M_1 = \frac{\alpha A(T_G)}{d_1 + cIL - bT_N}, \quad T_N = \frac{uM_1}{d_4}. \quad (15)$$

Using the equation for  $IL$  and  $T_N$  in equations (14) and (15) respectively, and substituting them into the formula for  $M_1$  in equation (15), the following quadratic equation is derived

<sup>3</sup> $\alpha$ ,  $\beta$  and  $\gamma$  are proportions of monocytes that differentiate into  $M_1$ ,  $M_2$  and  $M_R$  macrophages resp.  $b$  and  $h$  are increasing rates of  $M_1$  and  $M_2$  resp.  $c$  is decreasing rate of  $M_1$  by  $IL$ -10.  $d_1$ ,  $d_2$  and  $d_3$  are dying rates of  $M_1$ ,  $M_2$  and  $M_R$  resp.  $u$ ,  $k$  and  $w$  are production rates of  $T_N$ ,  $T_G$  and  $IL$ -10 resp.  $d_4$   $d_5$  and  $d_6$  are decay rate of  $T_N$ ,  $T_G$  and  $IL$ -10 resp.

<sup>4</sup>Changes were made in the parameter values in Table 1 and 2 to find out all the possible changes in the numerical solutions so the possible hypothesis can be made.

<sup>5</sup>The parameter values were adopted from the research work of other people [25, 24].

for  $M_1$ .

$$\frac{bu}{d_4}M_1^2 - \left( \frac{d_1d_3d_6 + cw\gamma A(T_G)}{d_3d_6} \right) M_1 + \alpha A(T_G) = 0. \quad (16)$$

This implies that  $M_1$  has two steady state solutions. Since  $T_N$  is expressed in terms of  $M_1$  (see equation 15),  $T_N$  also has two steady state solutions. Combining equation (8) and (11) we find an equation for  $T_G$ ,

$$A(T_G) = \frac{-hd_5}{\beta k}T_G^2 + \frac{d_2d_5}{\beta k}T_G \quad (17)$$

According to Waugh and Sherratt [25], the function  $A(T_G)$  is given by:

$$A(T_G) = -2.47T_G^3 + 21.94T_G^2 + 6.41T_G + 1.75 \quad (18)$$

Combining equations (17) and (18) and simplifying gives the following cubic equation in terms of  $T_G$ .

$$-2.47T_G^3 + \left( 21.94 + \frac{hd_5}{\beta k} \right) T_G^2 + \left( 6.41 - \frac{d_2d_5}{\beta k} \right) T_G + 1.75 = 0 \quad (19)$$

The solution of this cubic equation either gives one real root and two imaginary roots or three real roots depending upon the choice of parameter values. But the choice of parameter values in our case gave three real roots. All the three real roots for  $T_G$  were used to calculate the steady state solutions of the other variables in the system of differential equations.

### 3.1 Calculated Steady State Solutions

Tables 3 - 8 below show the calculated steady state solutions of all the six variables, in the system of differential equations, for each of the plots below (Figures 3-5, 8, 10 and 12) and Table 9 also shows MATLAB numerical values for  $t = 99$  ( $t$ =time in days), for all the six variables in the system of differential equations. Comparing the two sets of values for all the variables, there is not much difference between the calculated steady state solutions of the variables and MATLAB generated values for  $t = 99$ .



Variable	Figure 3
$M_1$ ( $cell\ mm^{-3}$ )	(46.5845, 2.3385), (34035.0773, 0.1297), (5.0063, -35425.9973)
$M_2$ ( $cell\ mm^{-3}$ )	(3.2240), (250.508), (1927.34)
$M_R$ ( $cell\ mm^{-3}$ )	(3.2040), (129.81173), (-5216.27)
$T_N$ ( $pg\ mm^{-3}$ )	(5.4805, 0.2751), (4004.1300, 0.0153), (0.5890, -4167.76)
$T_G$ ( $pg\ mm^{-3}$ )	(0.0248), (1.9270), (14.8257)
IL-10 ( $pg\ mm^{-3}$ )	(0.8778), (35.5694), (-149.11)

Table 3: Calculated Steady State Solutions for different set of parameters.

Variable	Figure 4
$M_1$ ( $cell\ mm^{-3}$ )	(44.3739, 2.9149), (629.5490, 9.3523), (2.0803, -6.6669)
$M_2$ ( $cell\ mm^{-3}$ )	(2.8690), (268.0328), (2024.1859)
$M_R$ ( $cell\ mm^{-3}$ )	(2.8532), (129.8760), (-3.0594)
$T_N$ ( $pg\ mm^{-3}$ )	(5.22046, 0.3429), (74.0646, 1.1003), (2.447 * 10 <sup>10</sup> , -0.7843)
$T_G$ ( $pg\ mm^{-3}$ )	(0.02207), (2.0618), (15.5707)
IL-10 ( $pg\ mm^{-3}$ )	(0.7817), (35.5824), (-8.388)

Table 4: Calculated Steady State Solutions for different set of parameters.

Variable	Figure 5
$M_1$ ( $cell\ mm^{-3}$ )	(41.0242, 3.8811), (612.6322, 14.1264), (14.6084, -33893.1634)
$M_2$ ( $cell\ mm^{-3}$ )	(2.3521), (297.6860), (2223.1200)
$M_R$ ( $cell\ mm^{-3}$ )	(2.3414), (127.2687), (-7281.2300)
$T_N$ ( $pg\ mm^{-3}$ )	(4.8264, 0.4566), (72.0744, 1.6619), (1.7186, -3987.4300)
$T_G$ ( $pg\ mm^{-3}$ )	(0.0181), (2.2899), (17.1009)
IL-10 ( $pg\ mm^{-3}$ )	(0.6415), (34.8682), (-106306)

Table 5: Calculated Steady State Solutions for different set of parameters.

Variable	Figure 8
$M_1$ ( $cell\ mm^{-3}$ )	(39.9486, 4.6467), (840.7917, 17.1693), (17.5225, -1.1624)
$M_2$ ( $cell\ mm^{-3}$ )	(1.3685), (371.3746), (3062.6954)
$M_R$ ( $cell\ mm^{-3}$ )	(2.2749), (176.9093), (-24959.9410)
$T_N$ ( $pg\ mm^{-3}$ )	(4.6998, 0.5467), (98.9167, 2.0199), (2.0615, -13674.7416)
$T_G$ ( $pg\ mm^{-3}$ )	(0.0105), (2.8567), (23.5592)
IL-10 ( $pg\ mm^{-3}$ )	(0.6233), (48.4683), (-6838.3400)

Table 6: Calculated Steady State Solutions for different set of parameters.

Variable	Figure 10
$M_1$ ( $cell\ mm^{-3}$ )	(2443.1440, 0.08545), (1467.9298, 17.4217), (17.6207, $-3.108722198 * 10^8$ )
$M_2$ ( $cell\ mm^{-3}$ )	(0.08773), (509.0210), (34856.1545)
$M_R$ ( $cell\ mm^{-3}$ )	(2.5438), (311.6137), (-6.6746)
$T_N$ ( $pg\ mm^{-3}$ )	(287.4290, 0.010053), (172.6980, 2.0496), (2.0730, $-3.65732 * 10^7$ )
$T_G$ ( $pg\ mm^{-3}$ )	(0.0006749), (3.9155), (268.1243)
IL-10 ( $pg\ mm^{-3}$ )	(0.6969), (85.3736), (-9.7449)

Table 7: Calculated Steady State Solutions for different set of parameters.

Variable	Figure 12
$M_1$ ( $cell\ mm^{-3}$ )	(38.4006, 0.2196), (65.3852, 0.9012), (1.8836, -1000.0189)
$M_2$ ( $cell\ mm^{-3}$ )	(11.4102), (95.5388), (1427.9036)
$M_R$ ( $cell\ mm^{-3}$ )	(0.9920), (6.9321), (-221.6060)
$T_N$ ( $pg\ mm^{-3}$ )	(4.5177, 0.02583), (7.6924, 0.1060), (0.2216, -117.6493)
$T_G$ ( $pg\ mm^{-3}$ )	(0.0878), (0.7349), (10.9839)
IL-10 ( $pg\ mm^{-3}$ )	(0.2718), (1.8992), (-60.7138)

Table 8: Calculated Steady State Solutions for different set of parameters.

Variable	Figure 3	Figure 4	Figure 5	Figure 8	Figure 10	Figure 12
$M_1$ ( $cell\ mm^{-3}$ )	2.3385	2.9149	3.8811	4.6467	5.1267	0.2196
$M_2$ ( $cell\ mm^{-3}$ )	3.2240	2.8690	2.3521	1.3685	0.0877	11.4103
$M_R$ ( $cell\ mm^{-3}$ )	3.2040	2.8532	2.3414	2.2749	2.5438	0.9920
$T_N$ ( $pg\ mm^{-3}$ )	0.2751	0.3429	0.4566	0.5467	0.6031	0.02583
$T_G$ ( $pg\ mm^{-3}$ )	0.02480	0.0221	0.0181	0.0105	0.0006749	0.08777
IL-10 ( $pg\ mm^{-3}$ )	0.87782	0.7817	0.6415	0.6233	0.6969	0.278

Table 9: Values, from MATLAB computations, for all the six variables when time,  $t = 99$

## 4 Numerical solution of equations

The model equations below were solved numerically using ode45, a non-stiff ODE solver in MATLAB.

$$\frac{dM_1}{dt} = \alpha A(T_G) + bT_N M_1 - cILM_1 - d_1 M_1 \quad (20)$$

$$\frac{dM_2}{dt} = \beta A(T_G) + hT_G M_2 - d_2 M_2. \quad (21)$$

$$\frac{dM_R}{dt} = \gamma A(T_G) - d_3 M_R. \quad (22)$$

$$\frac{dT_N}{dt} = uM_1 - d_4 T_N. \quad (23)$$

$$\frac{dT_G}{dt} = kM_2 - d_5 T_G. \quad (24)$$

$$\frac{dIL}{dt} = wM_R - d_6 IL. \quad (25)$$

While investigating the model equations, simulation of normal wound healing was obtained. An assumption was made that the  $M_1$  macrophages enter in the wound first before the  $M_2$  and  $M_R$  macrophages at the beginning of the inflammatory phase. The initial conditions,  $M_1(0) = 50 \text{ cell mm}^{-3}$ ,  $M_2(0) = 10 \text{ cell mm}^{-3}$ ,  $M_R(0) = 5 \text{ cell mm}^{-3}$ ,  $T_G(0) = 4 \text{ cell mm}^{-3}$ ,  $T_N(0) = 6 \text{ pg mm}^{-3}$  and  $IL(0) = 1 \text{ pg mm}^{-3}$  were chosen for the simulation. To simulate normal wound healing, it was assumed that  $\alpha = 1/3$ ,  $\beta = 1/3$  and  $\gamma = 1/3$  (i.e. the number of monocytes differentiating into  $M_1$ ,  $M_2$  and  $M_R$  macrophages are equal). This assumption was based on similar assumption made by Waugh, Helen V. and Jonathan A. Sherratt [25, 24]. The function  $A(T_G)$  that was used in the simulation is the same as the one illustrated in Figure 2. The profile for this simulation is illustrated in Figure 3. The numerical solutions in Figure 3 show that all the macrophages increase between day 1 and 2 initially to a point and then decrease to very low levels. Also, TNF and IL-10 which are produced by  $M_1$  and  $M_R$  macrophages increase between day 1 and 2 initially to a point and then decrease to very low levels. TGF- $\beta$ , which is produced by  $M_2$  macrophages start decreasing initially to low levels in day 1.

In Figure 4, these values were chosen:  $\alpha=0.4$ ,  $\beta=0.3$  and  $\gamma=0.3$  and all other parameter values and initial conditions are the same as in Figure 3 (i.e there is more monocytes

differentiating into  $M_1$  macrophages than  $M_2$  and  $M_R$  macrophages and the same number of monocytes differentiate into  $M_2$  and  $M_R$  macrophages). These values were chosen to investigate the possible changes in the plots of the variables so that possible hypothesis can be made. Both plots (Figure 3 and 4) are similar. But when  $\alpha = 0.5$ ,  $\beta = 0.25$  and  $\gamma = 0.25$  and all other parameter values and initial conditions are the same as in Figure 3, the plots (see Figure 5) are similar to the plots in Figure 3 except for the plot of  $M_1$  macrophages, (see Figure 5), which shows that the levels of  $M_1$  macrophages after day 15 is higher than the levels  $M_1$  macrophages after day 15 in Figure 3 and 4.

However, if  $\alpha = 0.5$ ,  $\beta = 0.3$ , (the proportion of monocytes that differentiate into  $M_2$  macrophage), and  $\gamma = 0.2$ , (the proportion of monocytes that differentiate into  $M_R$  macrophage), the numerical results show that  $M_1$  macrophages and TNF increase slightly between day 1 and 2 and start decreasing slowly after day 3. However, both plots increase exponentially after day 15. The plots for  $M_2$  and  $M_R$  macrophages, IL-10 and TGF- $\beta$  are similar to the plots in Figure 3.

In Figure 7,  $\alpha$  was increased to 0.6 and both  $\beta$  and  $\gamma$  were 0.2 (i.e 60% of monocytes become  $M_1$  macrophages and 20% each for both  $M_2$  and  $M_R$  macrophages). The other parameters and initial conditions are the same as in Figure 3. The numerical results show that  $M_1$  macrophages and TNF increase slowly between day 1 and 10 and then increase exponentially after day 10. However,  $M_2$  macrophages,  $M_R$  macrophages and IL-10 increase between day 1 and 2 and then decrease to low levels but TGF- $\beta$  start decreasing initially to very low levels. However, if  $\alpha = 0.6$ ,  $\beta = 0.15$  and  $\gamma = 0.25$  the numerical results, (see Figure 8), show that all the macrophage phenotypes increase between day 1 and 2 to a point and then decrease to low levels. Also TNF and IL-10 increase between day 1 and 2 to a point and then decrease to low levels, but TGF- $\beta$  start decreasing initially to very low levels.

In Figure 9,  $\alpha$  was increased to 0.7 and both  $\beta$  and  $\gamma$  were 0.15 (i.e 70% of monocytes become  $M_1$  macrophages and 15% each for both  $M_2$  and  $M_R$  macrophages). The other parameters and initial conditions are the same as in Figure 3. The numerical results show that  $M_1$  macrophages and TNF increase slowly between day 1 and 5 and then increase exponentially after day 5. However,  $M_2$  macrophage,  $M_R$  macrophage and IL-10 increase between day 1

and 2 and then decrease to low levels but TGF- $\beta$  start decreasing initially to very low levels. However, if  $\alpha = 0.6$ ,  $\beta = 0.01$  and  $\gamma = 0.29$  the numerical results, (see Figure 10), show that  $M_1$  and  $M_2$  macrophages increase between day 1 and 2 to a point and then decrease to low levels.  $M_2$  macrophage start decreasing initially to low levels. Also TNF and IL-10 increase between day 1 and 2 to a point and then decrease to low levels, but TGF- $\beta$  start decreasing initially to very low levels.

In Figure 11, Both  $\alpha$  and  $\gamma$  were decreased to 0.05 and  $\beta$  was increased to 0.9 (i.e 90% of monocytes become  $M_2$  macrophages and 5% each for both  $M_1$  and  $M_R$  macrophages). The other parameters and initial conditions are the same as in Figure 3. The numerical results show that  $M_1$  macrophages and TNF increase slowly between day 1 and 20 and then start increasing exponentially after day 20. However,  $M_2$  macrophage,  $M_R$  macrophage and IL-10 increase between day 1 and 2 and then decrease to low levels but TGF- $\beta$  start decreasing initially to very low levels. However, if  $\alpha = 0.02$ ,  $\beta = 0.9$  and  $\gamma = 0.08$  the numerical results, (see Figure 12), show that  $M_2$  and  $M_R$  macrophages increase between day 1 and 2 to a point and then decrease to low levels.  $M_1$  macrophage and TNF start decreasing initially to low levels. Also, IL-10 increase between day 1 and 2 to a point and then decrease to low levels, but TGF- $\beta$  start decreasing initially to very low levels.

Figures 3 - 12 show the profiles of macrophage phenotypes and the respective chemicals (cytokines) they produce. The numerical results show that all the variables, in the system of differential equations, decrease to low levels before day 20 except for Figure 6, 7, 9 and 11, where  $M_1$  macrophages and TNF increase exponentially after day 5.

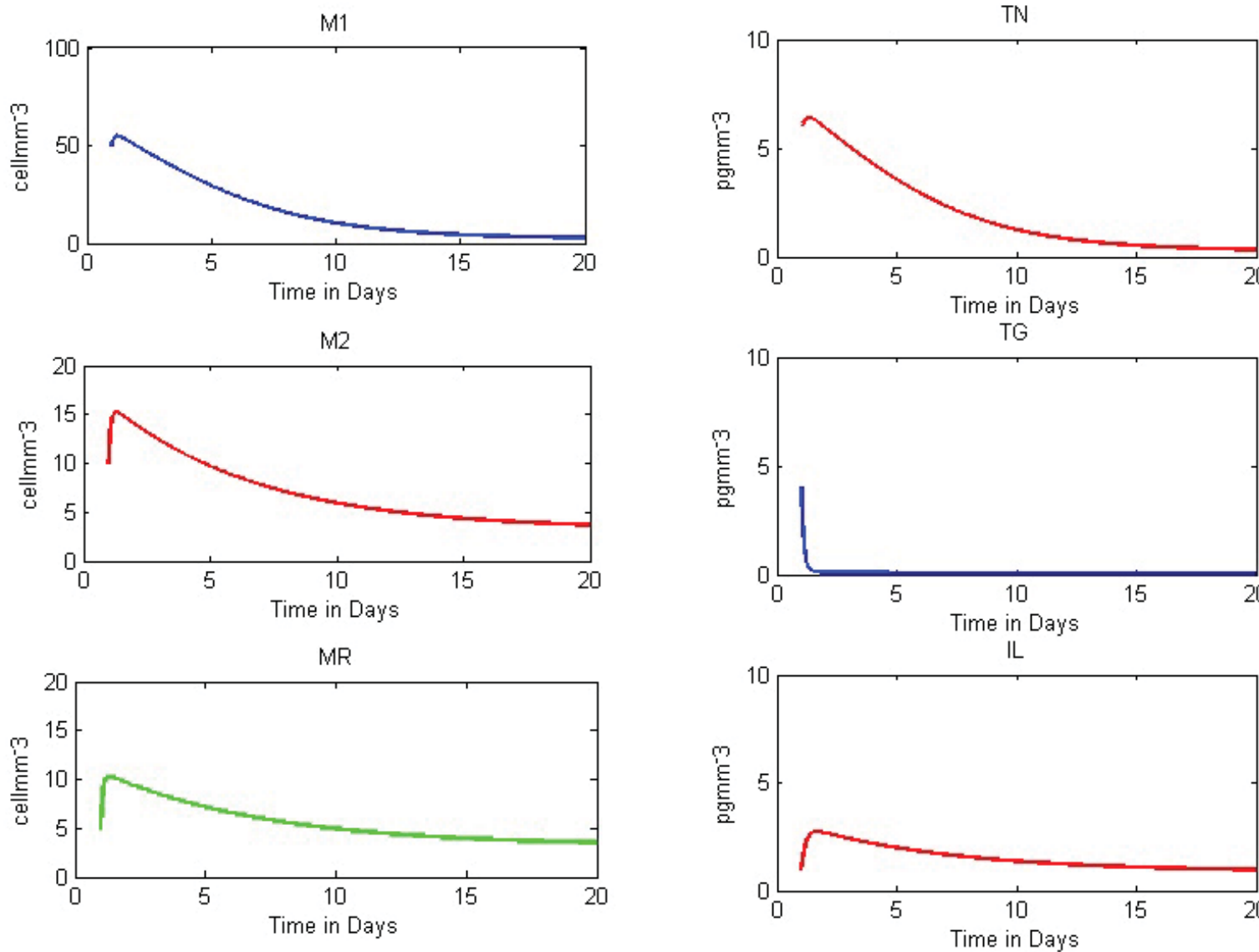


Figure 3: The initial conditions:  $M_1(0) = 50 \text{ cell mm}^{-3}$ ,  $M_2(0) = 10 \text{ cell mm}^{-3}$ ,  $M_R(0) = 5 \text{ cell mm}^{-3}$ ,  $T_G(0) = 4 \text{ cell mm}^{-3}$ ,  $T_N(0) = 6 \text{ pg mm}^{-3}$  and  $IL(0) = 1 \text{ pg mm}^{-3}$ . The parameters are:  $\alpha = 1/3$ ,  $\beta = 1/3$ ,  $\gamma = 1/3$ .

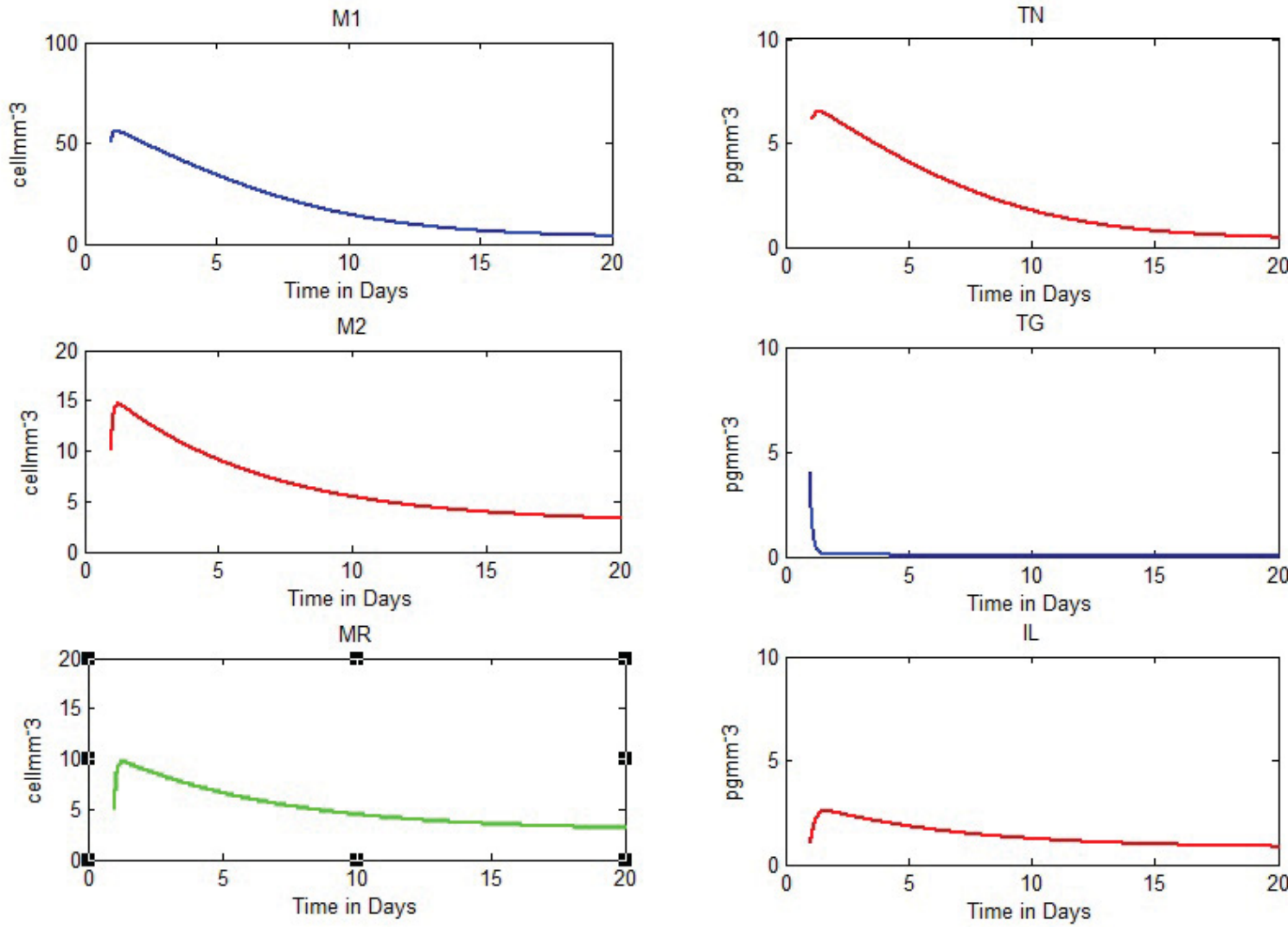


Figure 4: The initial conditions:  $M_1(0) = 50 \text{ cell mm}^{-3}$ ,  $M_2(0) = 10 \text{ cell mm}^{-3}$ ,  $M_R(0) = 5 \text{ cell mm}^{-3}$ ,  $T_G(0) = 4 \text{ cell mm}^{-3}$ ,  $T_N(0) = 6 \text{ pg mm}^{-3}$  and  $IL(0) = 1 \text{ pg mm}^{-3}$ . The parameters are:  $\alpha = 0.4$ ,  $\beta = 0.3$ ,  $\gamma = 0.3$ . All other parameters same as in Figure 3

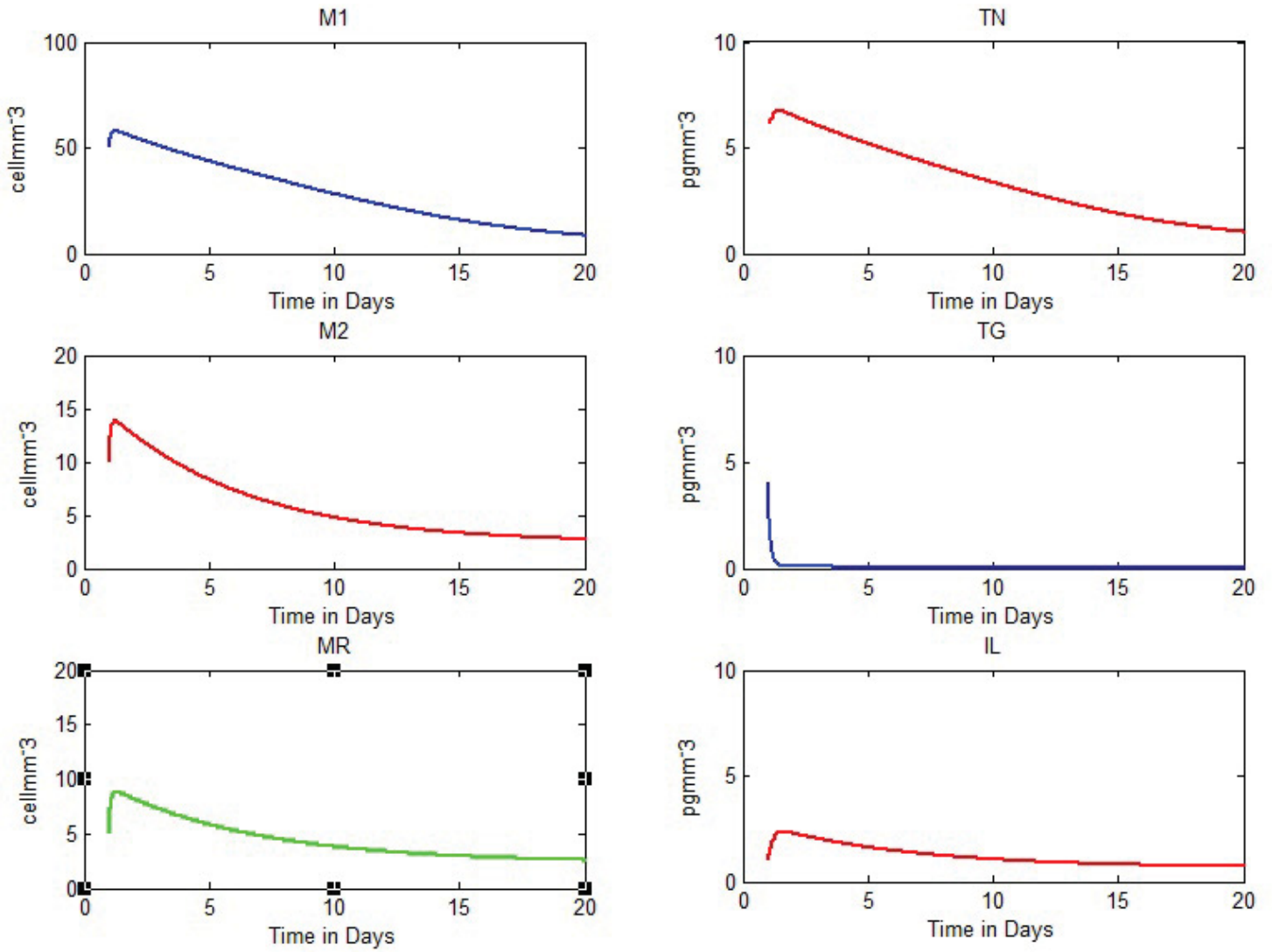


Figure 5: The initial conditions:  $M_1(0) = 50 \text{ cell mm}^{-3}$ ,  $M_2(0) = 10 \text{ cell mm}^{-3}$ ,  $M_R(0) = 5 \text{ cell mm}^{-3}$ ,  $T_G(0) = 4 \text{ cell mm}^{-3}$ ,  $T_N(0) = 6 \text{ pg mm}^{-3}$  and  $IL(0) = 1 \text{ pg mm}^{-3}$ . The parameters are:  $\alpha = 0.5$ ,  $\beta = 0.25$ ,  $\gamma = 0.25$ . All other parameters same as in Figure 3



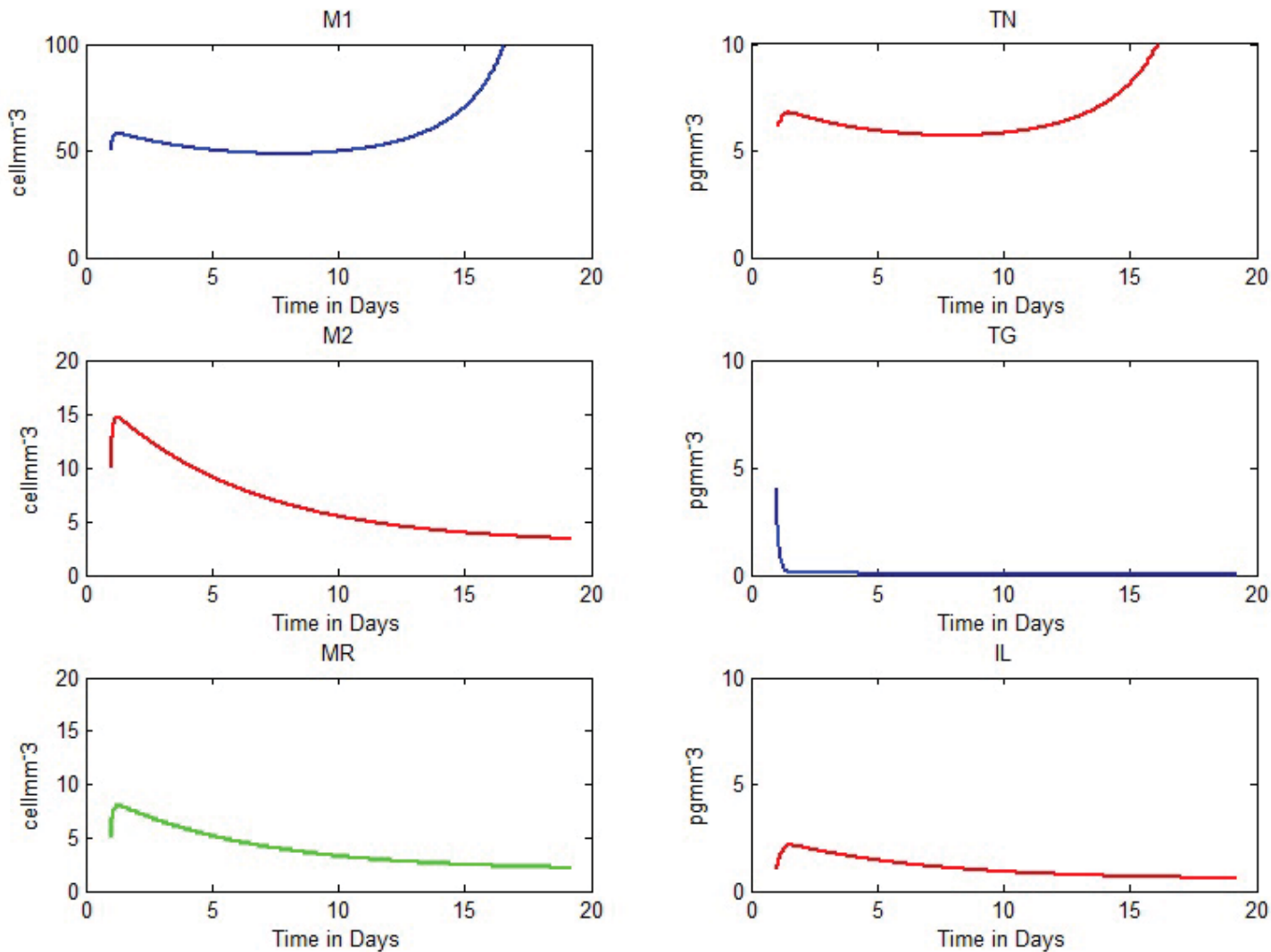


Figure 6: The initial conditions:  $M_1(0) = 50 \text{ cell mm}^{-3}$ ,  $M_2(0) = 10 \text{ cell mm}^{-3}$ ,  $M_R(0) = 5 \text{ cell mm}^{-3}$ ,  $T_G(0) = 4 \text{ cell mm}^{-3}$ ,  $T_N(0) = 6 \text{ pg mm}^{-3}$  and  $IL(0) = 1 \text{ pg mm}^{-3}$ . The parameters are:  $\alpha = 0.5$ ,  $\beta = 0.3$ ,  $\gamma = 0.2$ . All other parameters same as in Figure 5

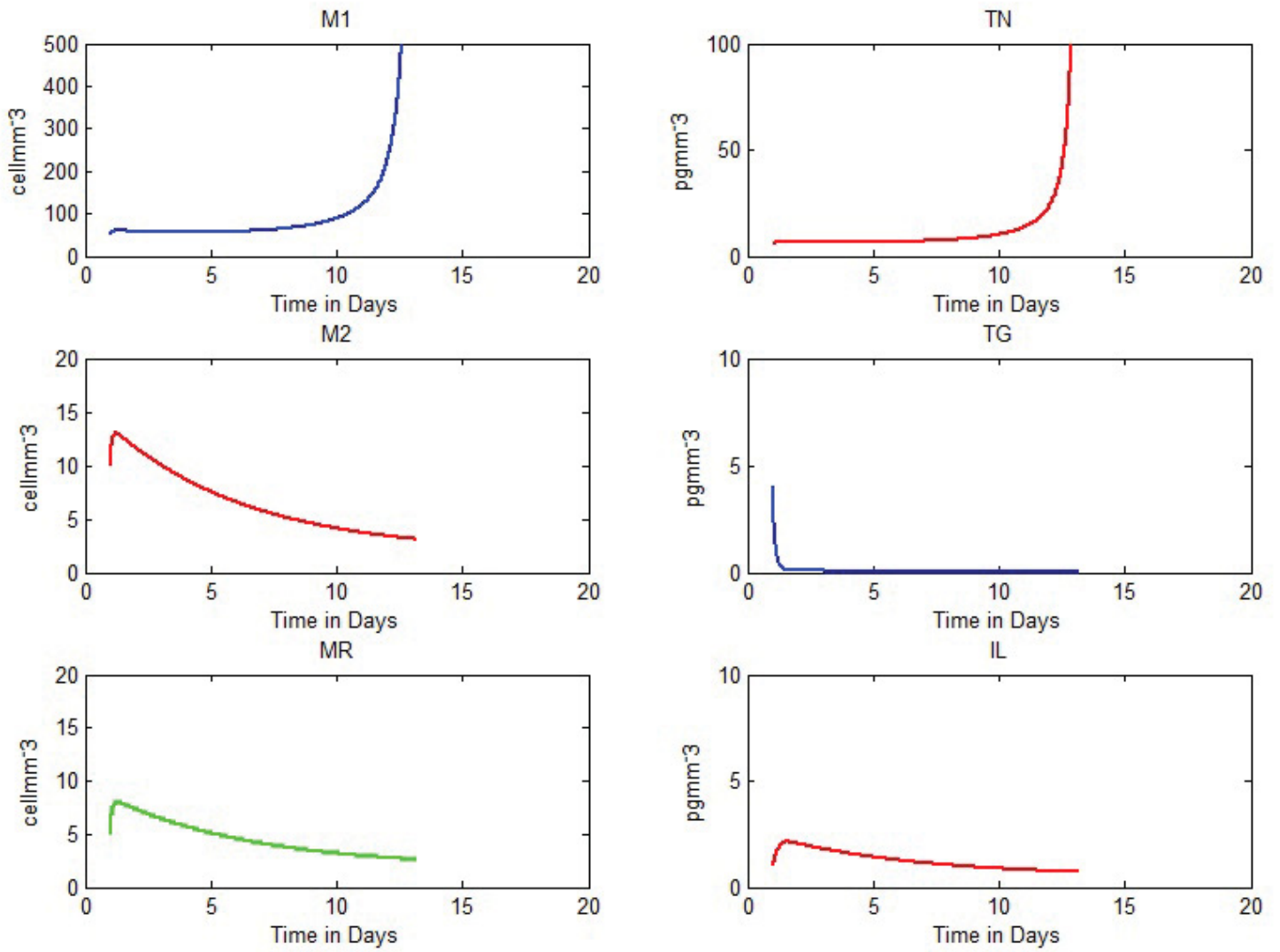


Figure 7: The initial conditions:  $M_1(0) = 50 \text{ cell mm}^{-3}$ ,  $M_2(0) = 10 \text{ cell mm}^{-3}$ ,  $M_R(0) = 5 \text{ cell mm}^{-3}$ ,  $T_G(0) = 4 \text{ cell mm}^{-3}$ ,  $T_N(0) = 6 \text{ pg mm}^{-3}$  and  $IL(0) = 1 \text{ pg mm}^{-3}$ . The parameters are:  $\alpha = 0.6$ ,  $\beta = 0.2$ ,  $\gamma = 0.2$ . All other parameters same as in Figure 3

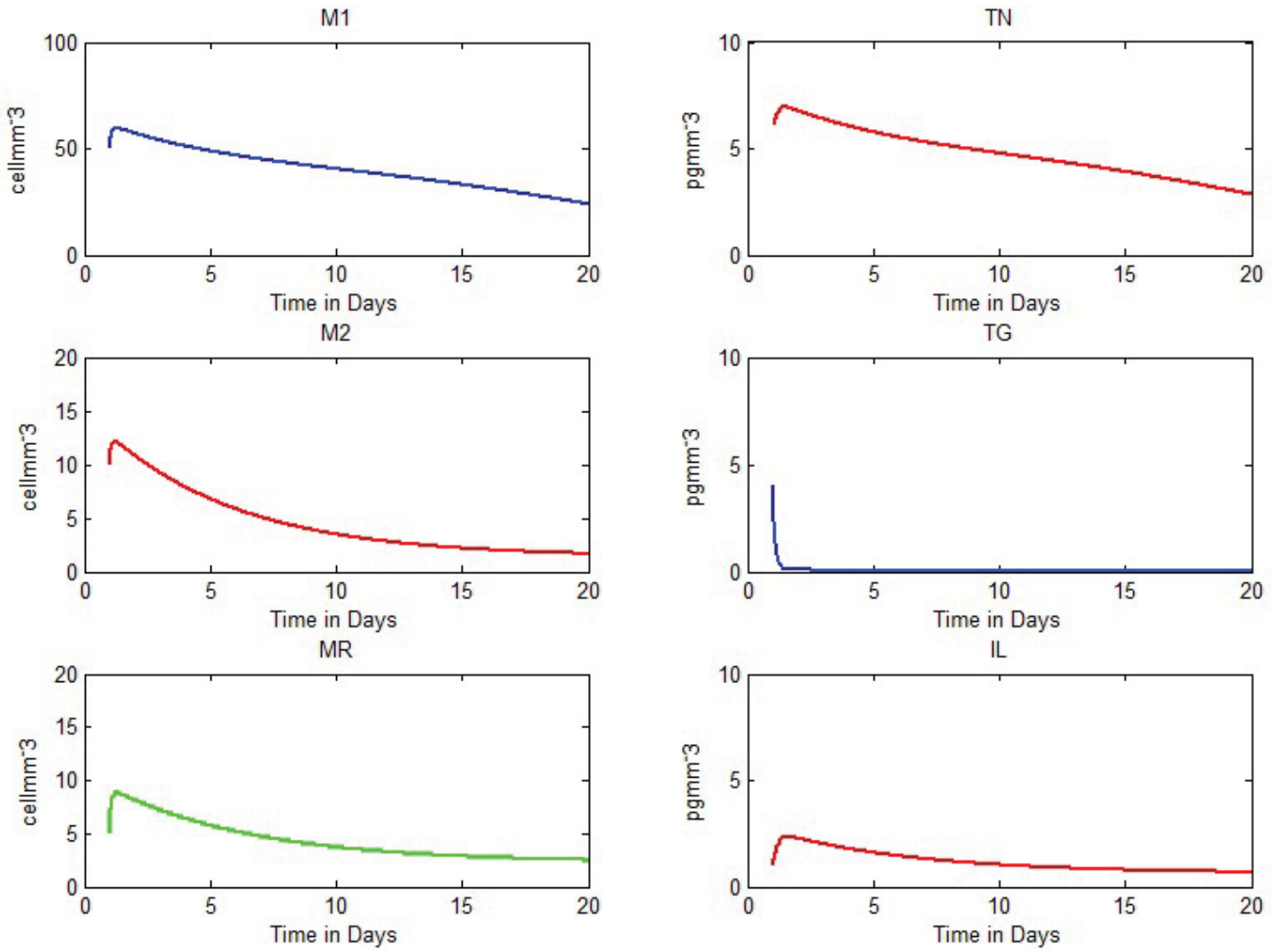


Figure 8: The initial conditions:  $M_1(0) = 50 \text{ cell mm}^{-3}$ ,  $M_2(0) = 10 \text{ cell mm}^{-3}$ ,  $M_R(0) = 5 \text{ cell mm}^{-3}$ ,  $T_G(0) = 4 \text{ cell mm}^{-3}$ ,  $T_N(0) = 6 \text{ pg mm}^{-3}$  and  $IL(0) = 1 \text{ pg mm}^{-3}$ . The parameters are:  $\alpha = 0.6$ ,  $\beta = 0.15$ ,  $\gamma = 0.25$ . All other parameters same as in Figure 7

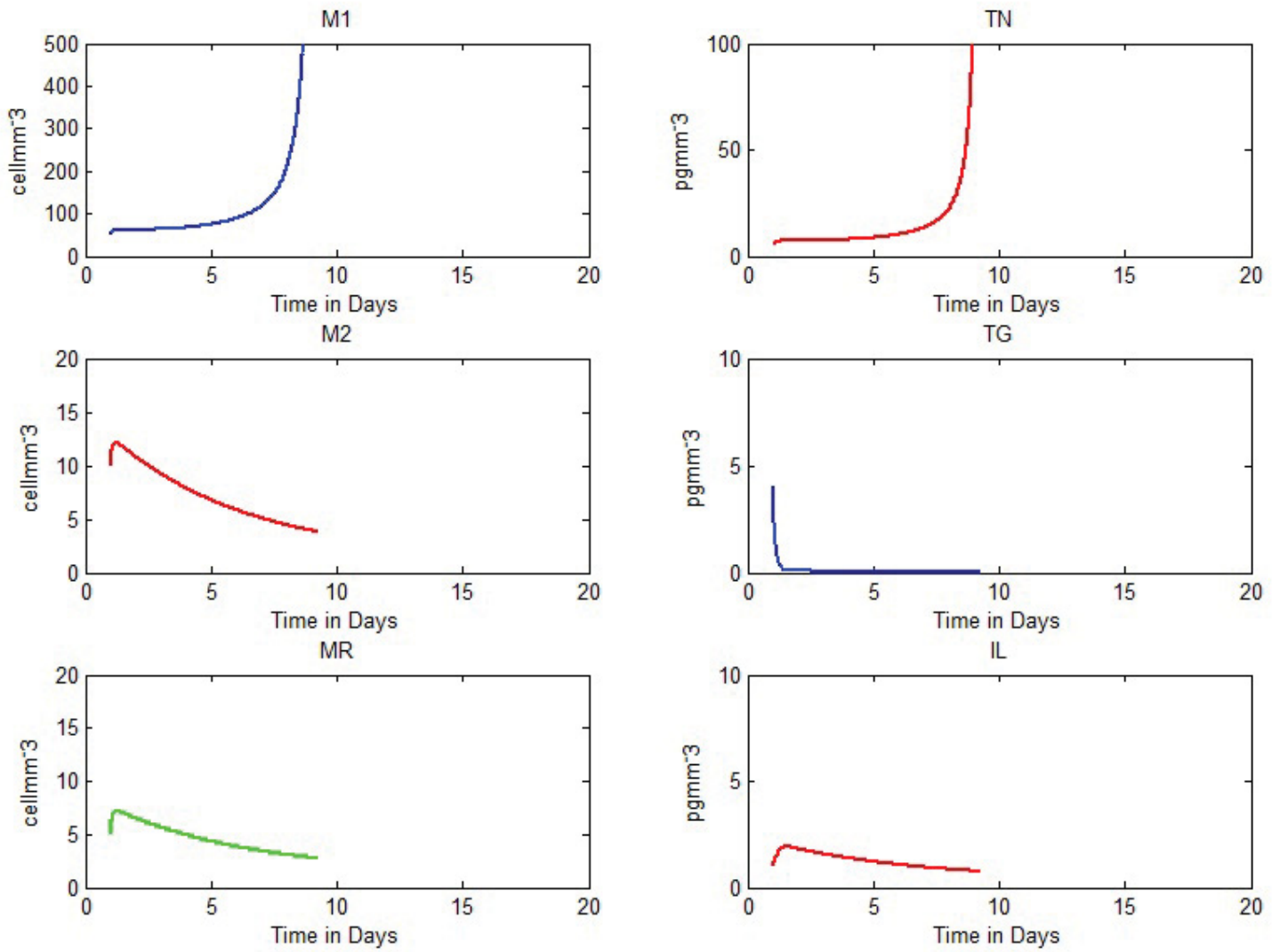


Figure 9: The initial conditions:  $M_1(0) = 50 \text{ cell mm}^{-3}$ ,  $M_2(0) = 10 \text{ cell mm}^{-3}$ ,  $M_R(0) = 5 \text{ cell mm}^{-3}$ ,  $T_G(0) = 4 \text{ cell mm}^{-3}$ ,  $T_N(0) = 6 \text{ pg mm}^{-3}$  and  $IL(0) = 1 \text{ pg mm}^{-3}$ . The parameters are:  $\alpha = 0.7$ ,  $\beta = 0.15$ ,  $\gamma = 0.15$ . All other parameters same as in Figure 3

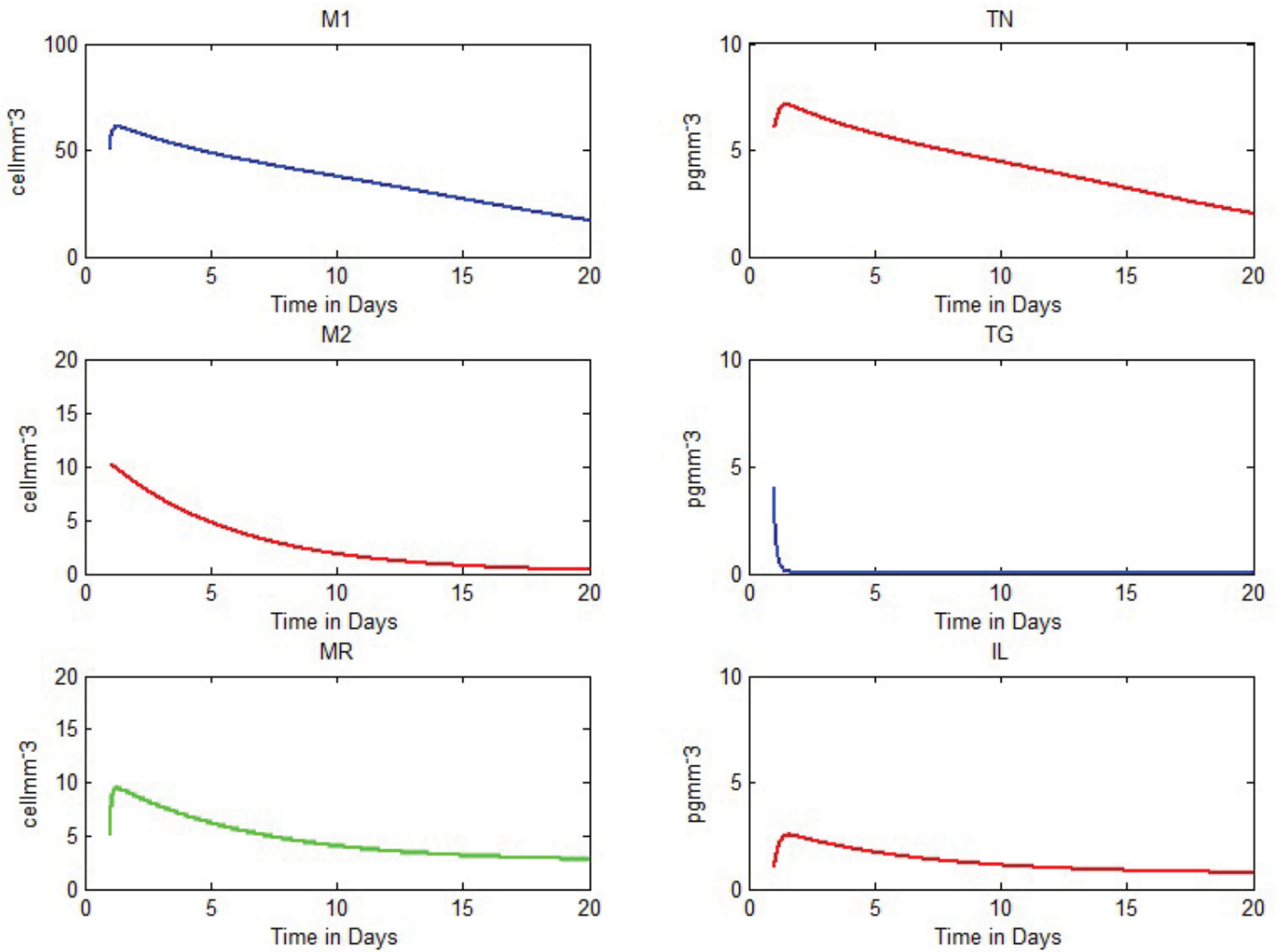


Figure 10: The initial conditions:  $M_1(0) = 50 \text{ cell mm}^{-3}$ ,  $M_2(0) = 10 \text{ cell mm}^{-3}$ ,  $M_R(0) = 5 \text{ cell mm}^{-3}$ ,  $T_G(0) = 4 \text{ cell mm}^{-3}$ ,  $T_N(0) = 6 \text{ pg mm}^{-3}$  and  $IL(0) = 1 \text{ pg mm}^{-3}$ . The parameters are:  $\alpha = 0.7$ ,  $\beta = 0.01$ ,  $\gamma = 0.29$ . All other parameters same as in Figure 9

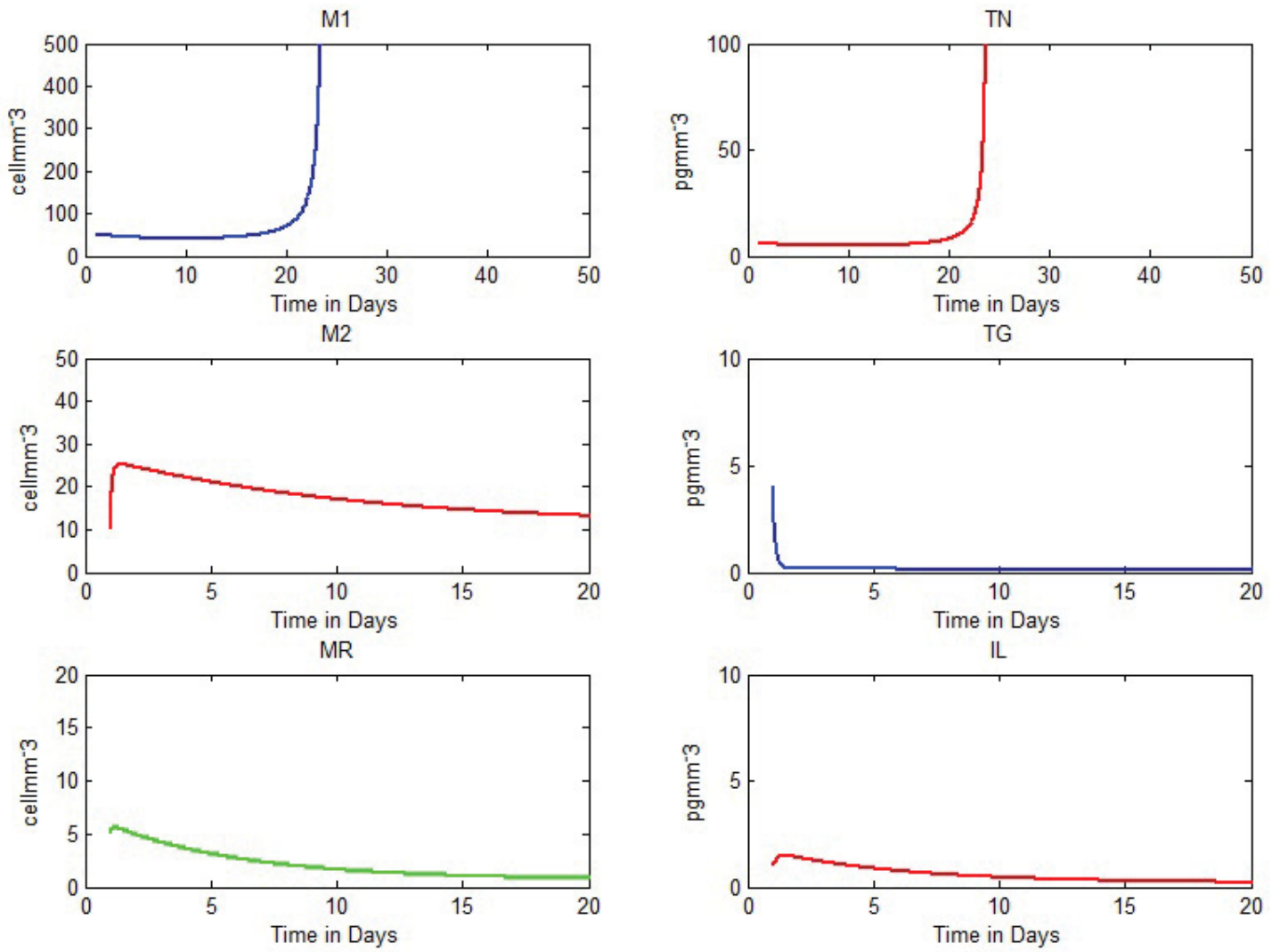


Figure 11: The initial conditions:  $M_1(0) = 50 \text{ cell mm}^{-3}$ ,  $M_2(0) = 10 \text{ cell mm}^{-3}$ ,  $M_R(0) = 5 \text{ cell mm}^{-3}$ ,  $T_G(0) = 4 \text{ cell mm}^{-3}$ ,  $T_N(0) = 6 \text{ pg mm}^{-3}$  and  $IL(0) = 1 \text{ pg mm}^{-3}$ . The parameters are:  $\alpha = 0.05$ ,  $\beta = 0.9$ ,  $\gamma = 0.05$ . All other parameters same as in Figure 3

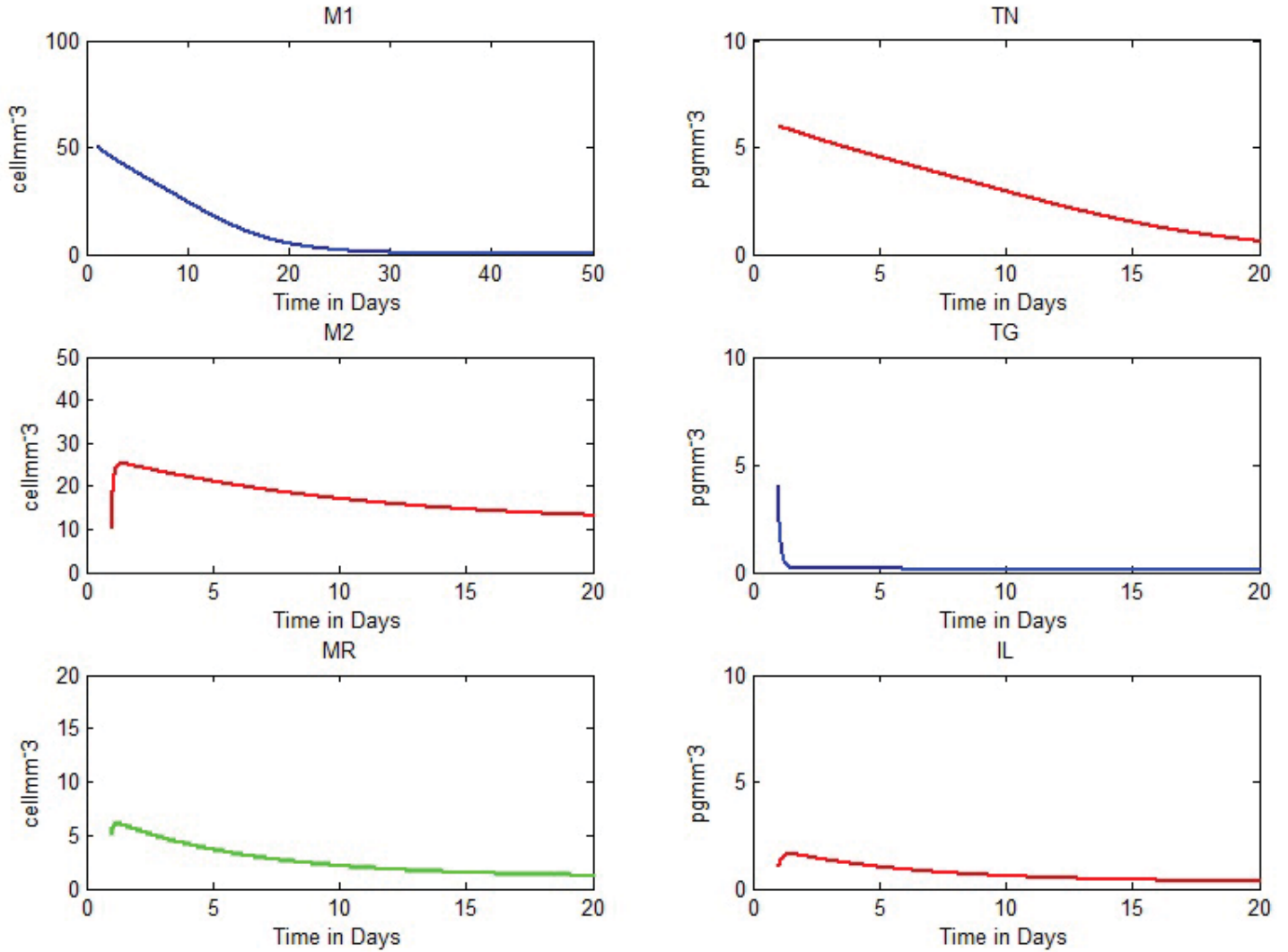


Figure 12: The initial conditions:  $M_1(0) = 50 \text{ cell mm}^{-3}$ ,  $M_2(0) = 10 \text{ cell mm}^{-3}$ ,  $M_R(0) = 5 \text{ cell mm}^{-3}$ ,  $T_G(0) = 4 \text{ cell mm}^{-3}$ ,  $T_N(0) = 6 \text{ pg mm}^{-3}$  and  $IL(0) = 1 \text{ pg mm}^{-3}$ . The parameters are:  $\alpha = 0.02$ ,  $\beta = 0.9$ ,  $\gamma = 0.08$ . All other parameters same as in Figure 11

## 5 Results and Discussion

The numerical solutions show that this model can give a clear explanation of normal wound healing, the numerical results, in Figures 3, 4 and 5, show that  $M_1$  macrophages increase between day 1 and 2 post injury and start decreasing to very low numbers in the wound after day 3 post injury. The calculated steady state solutions were compared with the values of  $M_1$  at  $t=99$  and there was not much difference. Refer to Table 3, 4, 5 and 9 for the

calculated steady state solutions and MATLAB solutions for  $M_1$ . The decreasing of  $M_1$  macrophages to very low levels after day 3 is very important to wound healing because inflammation ends after day 3 which implies that very high numbers of  $M_1$  macrophages in the wound after day 3 might result in more inflammation, since  $M_1$  macrophages are pro-inflammatory macrophages.

In Figure 5, where we assumed that 50% of monocytes differentiate into  $M_1$  and 25% each for  $M_2$  and  $M_R$ , the plot of  $M_1$  indicates that  $M_1$  macrophages linger in the wound for a longer time before leaving the wound site. This implies that there may be more inflammation in the wound, as long as there is an imbalance between  $M_1$  and  $M_R$  macrophages. This is consistent with the fact that higher numbers of pro-inflammatory macrophages in wounds causes more inflammation in the wound [24]. The concentration of TNF in the wound stimulates  $M_1$  macrophages. According to the numerical results of the model, TNF concentrations increases between day 1 and 2 post injury, and decreases to very low levels in the wound. This is known by comparing the calculated steady state solution of TNF with the MATLAB solution for TNF (see Table 5 and 9). This shows that the wound is healing since very high levels of TNF concentrations in the wound after inflammation might cause pro-inflammatory macrophages ( $M_1$  macrophages) to increase resulting in more inflammation, which is a sign of non-healing wound [25]. The TGF- $\beta$  causes monocytes to migrate into the wound and differentiate into  $M_1$ ,  $M_2$  and  $M_R$  macrophages. The decreasing trend of TGF- $\beta$  concentration in the wound, as time progresses, is regulated by the  $M_2$  macrophages in the wound. Reduction of TGF- $\beta$  is very important for normal wound healing, since more monocytes migration means more  $M_1$  macrophages which can be damaging to the wound if they are not regulated. However, if 50% of monocytes differentiate into  $M_1$ , 30% of monocytes differentiate into  $M_2$  macrophage and 20% of monocytes differentiate into  $M_R$ , the numerical results, in Figure 6, show macrophage the  $M_1$  macrophage and TNF increase exponentially after day 15. This implies that the wound is not healing since higher levels of  $M_1$  macrophages in wound causes more inflammation, which is a sign of non-healing wound. From the numerical results in Figure 5 and 6, it be said that wound may progress through the inflammatory phase successfully if there is sufficient amount of  $M_R$  macrophages in the wound. However,



the exponential increase of  $M_1$  and  $T_N$  (in Figure 6) has no biological meaning, since cells in the body do not proliferate exponentially. This implies that modifications of our model are needed to address this situation.

In Figure 7, an assumption was made that 60% of monocytes differentiate into  $M_1$  macrophages and 20% each for  $M_2$  and  $M_R$  macrophages. The numerical results show that  $M_1$  macrophages and TNF increase slowly between day 1 and 10 and then increase exponentially after day 10. However,  $M_2$  macrophage,  $M_R$  macrophage and IL-10 increase between day 1 and 2 and then decrease to low levels but TGF- $\beta$  start decreasing initially to very low levels. The higher levels of  $M_1$  macrophage and TNF show that there is more inflammation in the wound. However, if  $\alpha = 0.6$ ,  $\beta = 0.15$  and  $\gamma = 0.25$  the numerical results, (see Figure 8), show that all the macrophage phenotypes increase between day 1 and 2 to a point and then decrease to low levels. Also, TNF and IL-10 increase between day 1 and 2 to a point and then decrease to low levels, but TGF- $\beta$  start decreasing initially to very low levels. The decreasing of  $M_1$  macrophage and TNF to low levels after day 3 show that there is less inflammation, which is a sign of a healing wound. The numerical results in Figure 7 and 8 show that wound may still progress through the inflammatory stage successfully even if there is an imbalance between pro-inflammatory macrophages ( $M_1$  macrophages) and repair macrophages ( $M_2$  and  $M_R$  macrophages ) if there is significant amount of  $M_R$  macrophages in the wound.

In Figure 9,  $\alpha$  was increased to 0.7 and both  $\beta$  and  $\gamma$  were 0.15 (i.e 70% of monocytes become  $M_1$  macrophages and 15% each for both  $M_2$  and  $M_R$  macrophages). The numerical results show that  $M_1$  macrophages and TNF increase slowly between day 1 and 5 and then increase exponentially after day 5. However,  $M_2$  macrophage,  $M_R$  macrophage and IL-10 increase between day 1 and 2 and then decrease to low levels but TGF- $\beta$  start decreasing initially to very low levels. However, if  $\alpha = 0.6$ ,  $\beta = 0.01$  and  $\gamma = 0.29$  the numerical results (see Figure 10) show that  $M_1$  and  $M_R$  macrophages increase between day 1 and 2 to a point and then decrease to low levels.  $M_2$  macrophage start decreasing initially to low levels. Also, TNF and IL-10 increase between day 1 and 2 to a point and then decrease to low levels, but TGF- $\beta$  start decreasing initially to very low levels. The numerical results in Figure 9 and

10 show that wound may still progress through the inflammatory stage successfully even if there is an imbalance between pro-inflammatory macrophages ( $M_1$  macrophages) and repair macrophages ( $M_2$  and  $M_R$  macrophages) if there is significant amount of  $M_R$  macrophages in the wound.

In Figure 11, Both  $\alpha$  and  $\gamma$  were decreased to 0.05 and  $\beta$  was increased to 0.9 (thus 90% of monocytes become  $M_2$  macrophages and 5% each for both  $M_1$  and  $M_R$  macrophages). The other parameters and initial conditions are the same as in Figure 3. The numerical results show that  $M_1$  macrophages and TNF increase slowly between day 1 and 20 and then increase exponentially after day 20. However,  $M_2$  macrophage,  $M_R$  macrophage and IL-10 increase between day 1 and 2 and then decrease to low levels but TGF- $\beta$  start decreasing initially to very low levels. However, if  $\alpha = 0.02$ ,  $\beta = 0.9$  and  $\gamma = 0.08$  the numerical results, (see Figure 12), show that  $M_2$  and  $M_R$  macrophages increase between day 1 and 2 to a point and then decrease to low levels.  $M_1$  macrophage and TNF start decreasing initially to low levels. Also, IL-10 increase between day 1 and 2 to a point and then decrease to low levels, but TGF- $\beta$  start decreasing initially to very low levels. This shows that wound may progress through the inflammatory phase if there is more  $M_R$  macrophages in wound than  $M_1$  macrophages.

The numerical results in Figures 4, 5, 8 and 10 illustrate that wound may progress through the inflammatory phase successfully even if more monocytes differentiate into  $M_1$  macrophages than  $M_R$  and  $M_2$  macrophages in the wound provided there is significant amounts of  $M_R$  macrophages in the wound. Also, the numerical results in Figure 12 illustrate that wound may progress through the inflammatory phase successfully if more monocytes differentiate into  $M_R$  macrophages than  $M_1$  macrophages. This implies that the levels of  $M_R$  macrophages in the wound is very important during the inflammatory phase of wound healing. Since IL-10 concentrations in the wound inhibits the  $M_1$  macrophages and IL-10 is secreted by  $M_R$  macrophages, for wounds to progress successfully through the inflammatory phase, there has to be enough  $M_R$  macrophages in the wound.

This model has only investigated the behavior of macrophage phenotypes and the respective chemical (cytokines) they produce during the inflammatory phase of wound healing.

However, there are other different cell population and growth factors present during wound healing that were not included in the model because our study focuses on the inflammatory phase. Therefore this model can only claim to model the inflammatory phase of normal wound healing.

## 6 Conclusion

The numerical results indicates that wounds progress through the inflammatory phase successfully if, approximately, equal amounts of monocytes differentiate into  $M_1$ ,  $M_2$  and  $M_R$  macrophages in the wound. Also, wounds may progress through inflammatory phase if there is an imbalance between pro-inflammatory macrophages and repair or regulatory macrophages provided there is enough  $M_R$  macrophages in the wound. However, this may take longer time. The numerical results also indicate that  $M_R$  macrophages play a key role in the inflammatory phase of wound healing and since  $M_R$  macrophages produce  $IL-10$ , there must be significant levels of  $IL-10$  concentrations in the wound to ensure that the  $M_1$  macrophages decrease to low levels in the wound. The leaving of the  $M_1$  macrophages from the wound is very good sign that the wound is progressing through the inflammatory phase successfully. Since monocytes differentiate in  $M_2$  and  $M_R$  in presence of interleukin 4 and 13, for normal healing to occur, there has to be enough interleukin 4 and 13 in the wound to ensure more  $M_2$  and  $M_R$  macrophages in the wound to promote wound repair.

Our model can be extended to find out the stability and sensitivity analysis of the steady state solutions, which were not done in this study. There is also a possible extension of this model which could investigate the role that macrophage phenotypes  $M_1$ ,  $M_2$  and  $M_R$  play in diabetic wounds. Also, there could be further work on how these macrophage phenotypes influence the proliferation and remodeling phases of wound healing.

In conclusion, the model highlights the importance of macrophage phenotypes particularly  $M_R$  macrophages in the inflammatory phase of wound healing.

## References

- [1] Sharp A. and Clark J. Diabetes and its effects on wound healing. *Nursing Standard*, 45:41–47, 2001.
- [2] E. Agyingi, S. Maggelakis, and D. Ross. The effect of bacteria on epidermal wound healing. *Mathematical Modeling of natural phenomena*, 5(3):28–39, 2010.
- [3] E. Black. Decrease of collagen deposition in wound repair in type 1 diabetes independent of glycemic control. *Arch. Surg.*, 138(1):34–40.
- [4] Harold Brem and Marjana Tomic-Canic. Cellular and molecular basis of wound healing in diabetes. *Journal of clinical investigation*, 117:1219–1222, 2007.
- [5] J. P. Bulgrin. Nitric oxide synthesis is suppressed in steroid-impaired and diabetic wound. *Wounds*, 7(48-57).
- [6] G. Dow, A. Browne, and R.G. Sibbald. Infection in chronic wounds: Controversies in diagnosis and. *Ostomy/Wound Management*, 48(8):23–40, 1999.
- [7] S Enoch and D.J Leaper. Basic science of wound healing. *Surgery(Oxford)*, 23(2):37–81, 2005.
- [8] T.J Fahey, A Sadaty, W.G Jones, A Barber, B Smoller, and G.T Shires. Diabetes impairs the late inflammatory response to wound healing. *The Journal of Surgical Research*, 50(4):308–318, 1991.
- [9] Jennifer Flegg. *Mathematical Modeling of Chronic Wound Healing*. PhD thesis, Queensland University of Technology, 2009.
- [10] DiPietro L. A. Koh T. J. Inflammation and wound healing: the role of the macrophage. *Expert reviews in molecular medicine*, 13:e23.
- [11] Naude L. The practice and science of wound healing: history and physiology of wound healing. *Professional Nursing Today*, 14(3).

- [12] O. Lerman. Cellular dysfunction in the diabetic fibroblast: Impairment in migration, vascular endothelial growth factor production and response to hypoxia. *America Journal of pathology*, 1(162):303–312.
- [13] M. A. Loots. Difference in cellular infiltrate and extracellular matrix of chronic diabetic wounds and venous ulcer versus acute wounds. *J. Invest. Dermatology*, 111(5):850–857.
- [14] Vincent A. M. Biology of diabetic neuropathy. *Handbook of clinical neurology*, 115:591–606.
- [15] Yoo D. Danilkovitch-Miagkova A. Leroux M. A. Maxso S., Lopez E. A. Role of mesenchymal stem cells in wound repair. *Stem cells translational medicine*, 1:142–149.
- [16] Peter J. Murray and Thomas A. Wynn. Protective and pathogenic functions of macrophage subsets. *Nature Review Immunology*, 11:723–737.
- [17] Menke N.B., Ward K.R, Witten T.M, Bonchev D.G, and Diegelmann R.F. Impaired wound healing. *Clinics in Dermatology*, 25(1):19–25, 2007.
- [18] Diegelmann R.F and Evans M.C. Wound healing: An overview of acute, fibrotic and delayed healing. *Frontiers in bioscience : a journal and virtual library*, 9:283–289, 2004.
- [19] D. W. H Riches. *Macrophage involvement in wound repair, modelling and fibrosis*. 2nd edition.
- [20] Steed D. L. Franz M. G. Robson, M. C. Wound healing: Biological features and approaches to maximize healing trajectories. *Curr. probl. Surg.*, 38(2):65–140.
- [21] Robert F. Diegelmann Kevin R. Ward Segal, Rebecca A. and Angela Reynolds. A differential equation model of collagen accumulation in a healing wound. *Bulletin of mathematical biology*, 74(9):2165–2182.
- [22] A.J Singer and R.A Clark. Cutaneous wound healing. *New England Journal of Medicine*, 341(10):738–746, 1999.
- [23] S. M. Wahl. Transforming growth factor beta induces monocyte chemotaxis and growth factor production. *Proceedings of national Academic of science USA.*, 84(16):5788–5792.

- [24] Helen V. Waugh and Jonathan A. Sherratt. Modeling the effects of treating diabetic wounds with engineered skin substitutes. *Wound repair and regeneration*, 15(4):556–565.
- [25] Helen V. Waugh and Jonathan A. Sherratt. Macrophage dynamics in diabetic wound healing. *Bulletin of Mathematical Biology*, pages 197–207, 2006.